LOCA Mass and Energy Release Analysis

Code Applicability Report for US-APWR

Non-Proprietary Version

February 2008

Revision History

Revision	Page	Description
0	All	Original issue
1		This revision is primarily intended to replace a sample analysis in this report with the limiting case of the containment analyses for the loss-of-coolant accident described in the US-APWR design control document. Some validation studies based on the sample analysis are also revised for consistency, although the results remain unchanged. The replaced objects are as follows:
	2-16	- The figure of Steam Generator (Figure 2-5)
	3-16	- The peak pressure and vapor temperature in the sample analysis
	3-19	- The verification of advanced accumulator model built into SATAN-VI and WREFLOOD code (Table 3-3)
	3-21	- The main input description for sample analysis of mass and energy release (Table 3-5)
	3-26, 3-27	- The sensitivity analysis results on the steam/water mixing model at DVI (Figure 3-5 and Figure 3-6)
	3-32 to 3-39	- The sample analysis results (Figure 3-12 to Figure 3-19)
	C-4 to C-7	- The validation of the NR Model (Figure C-2 to Figure C-8)

Mitsubishi Heavy Industries, Ltd.
16-5, Konan 2-chome, Minato-ku
Tokyo 108-8215 Japan

ABSTRACT

The Standard Review Plan (Reference 1) states that LOCA mass and energy release evaluation analyses performed with the Appendix K ECCS computer codes which were developed to comply with the ECCS Acceptance Criteria presented in 10CFR50.46 and 10CFR50 Appendix K shall be acceptable. “Westinghouse LOCA Mass and Energy Release Model for Containment Design March 1979 Version (Reference 2)” conforms to the standard and is approved by the NRC.

In order to meet this standard while incorporating modified analytical models reflecting US-APWR new features, MHI has developed a modified mass and energy release model which is based on the ECCS Appendix K codes (SATAN-VI and WRFLOOD). Where applicable and appropriate, conservative models for mass and energy release calculations have been added into the codes.

A sample mass and energy release calculation, in which a double ended guillotine break at pump suction was assumed as postulated LOCA condition was performed by using the analytical models described above.

The methodology as presented will be used when determining maximum containment pressure and temperature following a loss-of-coolant accident for the US-APWR.

Table of Contents

List of Tables

List of Figures

List of Acronyms

ACC	Accumulator
APWR	Advanced Pressurized Water Reactor
CS	Containment Spray
CSS	Containment Spray System
CVCS	Chemical and Volume Control System
DNB	Departure from Nucleate Boiling
DVI	Direct Vessel Injection
ECCS	Emergency Core Cooling System
EPRI	Electric Power Research Institute
EPS	Emergency Power Source
ESF	Engineered Safety Feature
FA	Fuel Assembly
Fout	Core carryover rate fraction in the reflooding phase
ICIS	In-Core Instrumentation System
LOCA	Loss Of Coolant Accident
LP	Lower Plenum of reactor vessel
M&E	Mass and Energy
MSLB	Main Steam Line Break
NPSH	Net Positive Suction Head
NR	Neutron Reflector
PWR	Pressurized Water Reactor
PZR	Pressurizer
RCCA	Rod Cluster Control Assemblies
RCP	Reactor Coolant Pump
RCS	Reactor Coolant System
RHR	Residual Heat Removal
RV	Reactor Vessel
RVH	Reactor Vessel Head
RVI	Reactor Vessel Internal
RWSP	Refueling Water Storage Pit
SDV	Safety Depressurization Valve
SG	Steam Generator
SRP	Standard Review Plan
SRV	Safety Relief Valve
Tinlet	Primary coolant temperature at reactor vessel inlet nozzle
TDF	Thermal Design Flow
UP	Upper Plenum of reactor vessel
Vin	Core flooding rate in the reflooding phase

1.0 INTRODUCTION

This report documents the acceptability of use of analysis codes and methodologies approved for the existing Pressurized Water Reactor (PWR) in their application to the US-APWR. The US-APWR is an advanced PWR with improved design to enhance reliability while retaining many basic features of the existing four-loop PWR. Therefore the methodologies for the existing PWRs are applicable to the US-APWR with minor modifications for the improved features.

This report demonstrates the applicability of the PWR analysis codes and methodologies used for calculation of mass and energy release to the containment following a design basis loss-of-coolant accident (LOCA) to the US-APWR. The method as presented are intended for use when determining maximum containment pressure and temperature following a loss-of-coolant accident.

Chapter 2 presents an overview of the US-APWR plant design features related to the LOCA analyses to assist in understanding applicability of the approved methodologies for current PWRs to the US-APWR.

Chapter 3 addresses the codes and methodology used for the mass and energy release analysis. In Section 3.2, the mass and energy release model with minor modifications reflecting the improved features of the US-APWR for the blowdown and reflood phases are described. And in Section3.3, the mass and energy release model for the post-reflood phases are described.

Also, Section 3.4 presents a sample mass and energy release calculation result performed by using the analytical models described above and its containment response.

Chapter 4 summarizes the version of the mass and energy release evaluation model with minor modifications, which is based on the approved methodology and discusses the conclusions.

2.0 US-APWR PLANT DESIGN AND FEATURES

This section describes certain aspects of the US-APWR design in order to assist in the understanding the applicability of the approved methodologies for current PWRs to the US-APWR. The US-APWR features highly reliable prevention functions, well-established mitigation systems with active safety functions, and passive safety functions. The primary system design, loop configuration, and main components are similar to those of currently operating PWRs.

2.1 Main Specifications

The US-APWR is an advanced PWR of improved design to enhance reliability while retaining the basic features of existing 4-loop PWRs. The main specifications of the US-APWR in comparison with existing 4-loop PWRs in the U.S. are shown in Table 2-1.

2.2 Reactor and Core

2.2.1 General Features

The reactor configuration of the US-APWR is shown in Figure 2-1. Comparisons of core parameters between the US-APWR and US current 4-loop PWRs are shown in Table 2-2.

The fuel assemblies, rod cluster control assemblies, reactor vessel internals and thermal hydraulic design are described below.

2.2.2 Fuel Assemblies

The fuel assembly consists of the 264 fuel rods arranged in a square 17x17 array, together with 24 control rod guide thimbles, an in-core instrumentation guide tube, 11 grid spacers, and top and bottom nozzles. This design maintains the same grid spacing (approximately 18 inches) as the 17x17 fuel assembly design in current plants. This relatively shorter grid spacing provides greater margin to grid fretting and improves DNB performance in comparison with the widely used standard design of about 14 ft heated length and 10 grid design. Fuel assembly characteristics are shown in Table 2-3.

2.2.3 Reactor Vessel Internals

The arrangement of the reactor vessel internals (RVI) of the US-APWR is shown in Figure 2-1. The increased fuel element length in the US-APWR is enabled by the integration of the lower core plate and lower core support plate.

The coolant flows from the RV inlet nozzles down the annulus between the core barrel and the RV and then into a plenum at the bottom of the RV. The flow then turns and passes through the lower core support plate and into the core. After passing through the core, the coolant enters the upper plenum and then flows radially to the core barrel outlet nozzles. A small amount of coolant flows into the vessel head plenum from the annulus to cool the

vessel head area.

A neutron reflector (NR) is used in the US-APWR to improve neutron utilization and thus the fuel cycle cost, to reduce neutron irradiation of the RV, and to increase structural reliability by eliminating bolts in the high neutron flux region. The NR assembly is shown in Figure 2-2.

The NR is located between the core barrel and core, and lines the core cavity. The NR consists of ten thick stainless steel blocks. These blocks are aligned by alignment pins and fixed to the lower core support plate by tie rods and bolts. The top and bottom are supported and aligned by alignment pins that are welded to the core barrel.

The NR is cooled by up-flow through cooling holes in the blocks. The flow is sufficient to avoid coolant boiling and prevent excessive stress and thermal deflections of the blocks due to the gamma heating. The total core bypass flow is approximately 7.5% of total reactor coolant system (RCS) flow rate. It is relatively larger than the flow rate at a existing PWR plant so as to allow enough cooling for the NR and to keep the Reactor Vessel Head (RVH) coolant temperature at Tinlet.

2.3 Reactor Coolant System

2.3.1 General Features

The RCS consists of the RV, the steam generators (SGs), the reactor coolant pumps (RCPs), the pressurizer (PZR) and the reactor coolant pipes and valves. The flow schematic for the RCS is shown in Figure 2-3.

The reactor coolant flows through the hot leg pipes to the SGs and returns to the RV via the cold leg pipes and the RCPs. The PZR is connected to one hot leg via the surge line and to two cold legs via the spray lines.

The reactor coolant system, including connections to related auxiliary systems, constitutes the reactor coolant pressure boundary.

The reactor coolant system performs the following functions.

- Circulates the reactor coolant through the reactor core and transfers heat to the secondary system via the steam generators.
- Cools the core sufficiently to prevent core damage during reactor operation.
- Forms the reactor coolant pressure boundary, which functions as a barrier to prevent radioactive materials in the reactor coolant from being released to the environment.
- Functions as a neutron moderator and reflector and as a solvent for boron.
- Controls the reactor coolant pressure.

The RV, SGs, RCPs, and PZR are individually described below.

2.3.2 Reactor Vessel

The reactor vessel (RV), shown in Figure 2-4, is a vertical cylindrical vessel with hemispherical top and bottom heads. The top head is a removable flanged closure head connected to the RV upper shell flange by stud bolts. Pads on the RV nozzles support the vessel.

The RV has four inlet nozzles, four outlet nozzles and four Direct Vessel Injection (DVI) nozzles, which are located between the upper reactor vessel flange and the top of the core, so as to maintain coolant in the reactor vessel in the case of leakage in the reactor coolant loop.

2.3.3 Steam Generators

The SGs, shown in Figure 2-5, are vertical shell U-tube evaporators with integral moisture separating equipments.

The design of the SGs for the US-APWR has been improved to attain high efficiency and reliability by adopting 3/4 inch (19.05 mm) outer diameter tubes made of alloy 690 thermal treated, which are arranged triangularly in 1 inch (25.4mm) pitch.

The reactor coolant enters the tube inlet plenum via the hot side primary coolant nozzle, flows through the inverted U-tubes, transferring heat from the primary side to the secondary side, and leaves from the SG lower head via the cold side primary coolant nozzle. The lower head is divided into inlet and outlet chambers by a vertical partition plate extending from the apex of the lower head to the tube sheet.

Steam generated on the shell side (secondary side) flows upward and exits through the outlet nozzle at the top of the vessel. Feedwater enters the steam generator at an elevation above the top of the U-tubes through a feedwater nozzle. The feedwater enters a feedring and is distributed through nozzles attached to the top of the feedring.

2.3.4 Reactor Coolant Pumps

The reactor coolant pumps (RCPs) for the US-APWR are upsized versions of the Type 93A pumps used in existing Westinghouse’s design PWRs. Their design is similar to that of the Type 93A RCPs.

The RCPs of US-APWR, shown in Figure 2-6, are vertical, single-stage, centrifugal, shaft seal units, driven by three-phase induction motors. The shaft is vertical with the motor mounted above the pump. A flywheel on the shaft above the motor provides additional inertia to extend pump coastdown. The pump suction is at the bottom, and the discharge is located on the side.

The reactor coolant that enters from the bottom of the casing is accelerated by the impeller and causes a pressure increase across the diffuser. The diffuser is located at the center of the casing in order to attain high hydraulic efficiency.

The US-APWR reactor coolant pump has achieved larger capacity and higher efficiency than those of Type 93A pump by improving of the impeller and diffuser configuration.

2.3.5 Pressurizer

The pressurizer (PZR), shown in Figure 2-7, is a vertical, cylindrical vessel with hemispherical top and bottom heads. The PZR is connected to one hot leg of the reactor coolant loops via the surge line and to two cold legs via the spray lines.

Electrical immersion heaters in the bottom head and the spray nozzle located in the top head control the primary system pressure.

The relief and safety valves at the top head provide overpressure protection of the RCS. The overpressure protection function of the US-APWR is performed as follows.

- Spring-loaded safety relief valves (SRVs) are installed on separate relief lines at the top of the pressurizer.
- An additional relief line has motor-operated relief valves for safety depressurization valves (SDVs). The valves are arranged in parallel and are driven by motor operators. A remotely controlled, motor-operated isolation valve is installed upstream of each the SDVs to allow isolation in the event of a leak.
- The relief lines discharge through spargers in the refueling water storage pit (RWSP) inside the containment.
- Safety relief valves are installed in the each residual heat removal system to provide overpressurization protection for unacceptable combinations of high reactor coolant system pressure and low reactor coolant system temperature.

2.4 Engineered Safety Features

2.4.1 General Features

The engineered safety features (ESFs) serve to mitigate the consequences of a design basis accident in which radioactive fission products are released from the reactor coolant system. The ESFs consist of the emergency core cooling system (ECCS), containment spray system (CSS), containment system, annulus air cleanup system and main control room heat, ventilation and air conditioning system.

The simplified configuration of the ECCS and CSS is shown in Figure 2-8.

The US-APWR employs the following advanced technologies for the ECCS and CSS to enhance its simplification.

a. Four-train, Direct Vessel Injection for High Head Injection System

The US-APWR employs a 4-train direct vessel injection (DVI) system. This system configuration increases redundancy and independence, and enhances safety and reliability. The capacity of each train is 50% of the capacity of a single train of a conventional two train system. Inter-connecting piping between each train is also eliminated.

The support system and the emergency AC power supply system also adopt a 4-train

configuration to enhance the reliability of the system.

b. Emergency Water Storage inside the Containment

The US-APWR eliminates potentially high risk operator actions to realign the suction in an emergency such as a Loss of Coolant Accident (LOCA) by installing the Refueling Water Storage Pit (RWSP) inside the containment. The RWSP is formed with a lined concrete structure and works as the emergency water source. This design significantly contributes to lowering the estimated core damage frequency.

c. Passive Low Head Injection

The safety system of the US-APWR consists of an optimized combination of active and passive components. The advanced accumulator is a passive component employed to enhance safety by improving flow injection characteristics and eliminating the need of the low head injection system. By adopting the vortex damper mechanism, the advanced accumulator supplies water with a large flow rate at the early stage of LOCA, and lower flow rate at the later stages.

The ECCS, CSS and containment system are described below.

2.4.2 Emergency Core Cooling System

The ECCS, shown in Figure 2-9, includes the accumulator system, high head injection system and emergency letdown system. The ECCS injects borated water into the reactor coolant system following a postulated accident and performs the following functions;

- Following a loss-of-coolant accident, the ECCS cools the reactor core, prevents serious damage to the fuel and fuel cladding, and limits the zirconium-water reaction in the fuel cladding to a very small amount.
- Following a main steam line break (MSLB), the ECCS provides negative reactivity to shut down the reactor.
- In the event that the normal CVCS letdown and boration capability are lost, the ECCS provides emergency letdown and boration of the RCS to orderly shutdown the reactor.

Compliance of the US-APWR ECCS with the 10 CFR 50.46 acceptance criteria is evaluated by ECCS Performance Analysis.

The ECCS design is intended to accomplish the following functions;

- In combination with control rod insertion, the ECCS is designed to shut down and cool the reactor during the following accidents;
  - Small break loss-of-coolant accidents
  - Control rod ejection
  - Main steam line break
  - Steam generator tube rupture
- The ECCS is designed with sufficient redundancy (four trains) to accomplish the specified safety functions assuming a single failure of an active component in the short term following an accident with one train out of service for maintenance, or a single failure of an active component or passive component for the long term following an accident with one train out of service.
- The emergency power source supply electrical power to the essential components of the ECCS, so the design functions are maintained during a loss of offsite power.

- The ECCS is automatically activated by a safety injection signal.
- The ECCS design permits periodical tests and inspections to verify integrity and operability.

2.4.2.1 Accumulator System

The accumulator system stores borated water under pressure and automatically injects it if the reactor coolant pressure decreases significantly. The accumulator system consists of four accumulators and the associated valves and piping, one for each RCS loop. The system is connected to the cold legs of the reactor coolant piping and injects borated water when the RCS pressure falls below the accumulator operating pressure. The system is passive. Pressurized nitrogen gas forces borated water from the tanks into the RCS.

As shown in Figure 2-10 accumulators incorporate internal passive flow dampers and a stand pipe which function to inject a large flow to refill the reactor vessel in the first stage of injection, and then reduce the flow as the water level in the accumulator drops. When the water level is above the top of the standpipe, water enters the flow damper through both inlets at the top of the standpipe and at the side of the flow damper such that water is injected at a large flow rate. When the water level drops below the top of the standpipe, water enters the flow damper only through the side inlet, so that accumulator injects water at a relatively low flow rate.

The accumulators provide large flow injection to refill the reactor vessel and continue with small flow injection during core reflooding in conjunction with the safety injection pumps. The combined performance of the accumulator system and the high head injection system eliminate the need for a conventional low head injection system. The accumulator system's performance for the US-APWR is shown in Figure 2-10.

2.4.2.2 High Head Injection System

The direct vessel injection (DVI) is employed for the high head injection system. The high head injection system consists of four independent trains, each containing a safety injection pump and the associated valves and piping. The safety injection pumps start automatically upon receipt of the safety injection signal. One of four independent safety electrical buses is available to each safety injection pump.

The safety injection pumps are aligned to take suction from the refueling water storage pit and to deliver borated water to the DVI nozzles on the reactor vessel. Two safety injection trains are capable of meeting the design cooling function for a Large Break LOCA, assuming a single failure in one train and another train out of service for maintenance. In the existing PWRs, the requirement for a Large Break LOCA is met through a low head injection pump that generally serves also as an RHR pump. Therefore, the capacity of the US-APWR high head injection pump is larger than the conventional high head pump in order to provide sufficient flow during the large break LOCA.

The refueling water storage pit in the containment provides a continuous borated water source for the safety injection pumps, thus eliminating the need for realignment from the refueling water storage pit to the containment sump.

2.4.3 Containment Spray System

The containment spray system (CSS), shown in Figure 2-11, consists of four independent trains, each containing a containment spray/residual heat removal (CS/RHR) heat exchanger, a CS/RHR pump, spray nozzles, piping and valves. The CS/RHR heat exchangers and the CS/RHR pumps are used for both CSS and RHRs function. The CSS sprays borated water into the containment vessel in the event of a loss-of-coolant accident.

The containment spray system functions to maintain the containment vessel internal peak pressure below the design pressure and reduce it to approximately atmospheric pressure in the event of a loss of coolant accident or a main steam line break.

The CSS is designed based on the following.

- Its safety functions can be accomplished if there is a single failure of an active component for a short term following an accident with one train out of service for maintenance, or a single failure of an active component or a single failure of a passive component for a long term following an accident with one train out of service for maintenance.
- The emergency power source can supply electrical power to the essential equipment of the CSS, so that safety functions can be maintained during a loss of offsite power.
- The CSS is automatically initiated by a containment spray signal.
- The CSS design permits periodic tests and inspections to verify integrity and operability.
- The CSS is capable of reducing the containment pressure to less than 50% of the peak calculated pressure for the design basis loss-of-coolant accident within 24 hours after the postulated accident.

The CSS is automatically actuated on receipt of a containment spray signal. When the signal is received, the CS/RHR heat exchanger outlet valves open and the CS/RHR pumps start. The CS/RHR pump motor is connected to a safety bus, so the emergency power source can supply electrical power in case of a loss of offsite power. The CS/RHR pumps take suction from the refueling water storage pit, and the stop valve on the inlet line is always open during reactor operation. The spray water is cooled by the CS/RHR heat exchangers and is delivered to the spray headers located in the top of the containment vessel.

The refueling water storage pit (RWSP) in the containment provides a continuous suction source for the CS/RHR pumps, thus eliminating the need for realignment from the refueling water storage pit to the containment sump.

The safety system pumps (CS/RHR pumps and safety injection pumps), which require sufficient net positive suction head (NPSH) to draw water from the recirculation sumps inside the containment, are located at the lowest level of the reactor building to secure the required NPSH. Also, they are located adjacent to the containment to minimize pipe lengths.

2.4.4 Containment System

The containment system includes the containment vessel, the annulus enclosing the

containment penetration area, and the containment isolation function performed by the isolation valves, airlocks and equipment hatch.

The containment system provides an effective leak-tight barrier and environmental radiation protection under all postulated conditions, including a loss-of-coolant accident.

2.4.4.1 Containment Vessel

The containment vessel is designed to completely enclose the reactor and reactor coolant system and to ensure that essentially no leakage of radioactive materials to the environment would result even if a major failure of the reactor coolant system were to occur. The configuration of containment vessel is shown in Figure 2-12.

The containment vessel consists of a prestressed, post-tensioned concrete structure with a cylindrical wall, a hemispherical dome, and a flat reinforced concrete foundation slab. The inside surface of the structure is lined with carbon steel.

The design pressure and temperature of the containment vessel are defined by the following postulated accidents.

- Loss- of-coolant accident (LOCA)
- Main steam line break (MSLB)

The containment vessel is designed to contain the energy and radioactive materials that result from a postulated loss-of-coolant accident, and for an 68 psig internal pressure to ensure a high degree of leak tightness during normal operation and under accident conditions.

An internal polar crane is supported by the containment vessel. A continuous crane girder transfers the polar crane loads to the containment vessel wall.

Hydrogen igniters are provided for protection against possible detonation following a core damage accident.

2.4.4.2 Refueling Water Storage Pit

The refueling water storage pit (RWSP) is located in the lowest part of the containment vessel. The RWSP provides a continuous suction source for both the safety injection pumps and the CS/RHR pumps. The wall and the floor of the RWSP are lined with stainless steel liner plates. The RWSP has four recirculation sumps on the floor; these sumps are provided with recirculation screens.

Table 2-1 Comparison of Principal Parameters

Parameter	US-APWR	US Current 4-loop PWR	Ratio
Core Thermal Output (MWt)	4,451	3,565 (3853)	1.25
Operation Pressure (psia)	2,250	2,250 (2250)	-
Hot Leg Temperature (deg. F)	617	620 (626)	-
Cold Leg Temperature (deg. F)	551	557 (559)	-
Thermal Design Flow (gpm/loop)	112,000	93,600	1.20
Number of Fuel Assembly	257	193 (193)	1.33
Fuel Assembly Lattice	17x17	17x17	-
Effective Fuel Length (ft)	14	12 (14)	-
Number of Fuel Rods per FA	264	264	-
Average Linear Heat Rate (kW/ft)	4.6	5.7 (5.2)	0.8
Number of RCCAs	69	53 (57)	1.30
Number of Control Rods per RCCA	24	24 (24)	-
SG Heat Transfer Area (ft^2)	91,500	55,000	1.66
PZR Volume (ft^3)	2,900	1,800	1.6
PZR Volume to Thermal Power (ft^3/MWt)	0.65	0.50	1.3
Containment Design Pressure (psig)	68	52 (56.5)	-

Vogtle Unit #1 are referred to as a US current 4-loop PWR.
Data in parentheses are those of South Texas Project Unit 1 and 2, current 4-loop PWR using 14-ft fuel. They are in the database of International Nuclear Safety Center and last updated on 01/97.

Table 2-2 Key Parameters of Core Design

Parameter	US-APWR	US Current 4-loop PWR
Core Thermal Output	4,451 MWt	3,565MWt
Heat Generated in Fuel	97.4 %	97.4 %
Number of Fuel Assemblies	257	193
Fuel Assembly Lattice	17x17	17x17
Effective Fuel Length	14 ft	12 ft
Average Linear Heat Rate	4.6 kW/ft	5.7 kW/ft
Primary System Pressure	2,250 psia	2,250 psia
Thermal Design Flow (TDF)	448,000 gpm	374,400 gpm
Coolant Temperature		
Hot Leg	617 °F*	620 °F*
RV Average	584 °F*	588 °F*
Cold Leg	551 °F*	557 °F*
Core Bypass Flow	7.5 %**	6.3 %

* Given as approximate figures
** Nominal value for DNBR analysis

Table 2-3 Fuel Assembly Specification

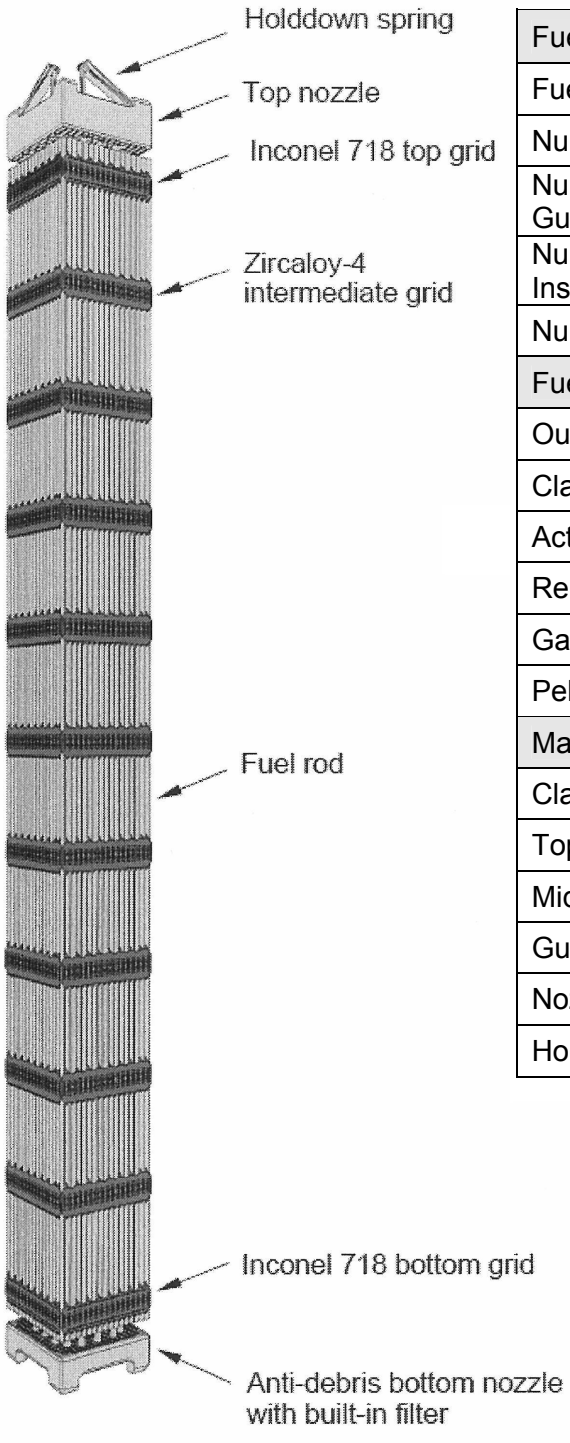

Fuel Assemblies	
Fuel Rods Array	17 x 17
Number of Fuel Rods	264
Number of Control Rod Guide Thimbles	24
Number of In-core Instrumentation Guide Tube	1
Number of Grid Spacers	11
Fuel Rods	
Outside Diameter	0.374 in. (9.50mm)
Cladding Thickness	0.022 in. (0.57mm)
Active Fuel Length	165.4" (4,200mm)
Reload Fuel Enrichment	Max. 5 wt%
Gadolinia Content	Max. 10 wt%
Pellet Density	97 %TD
Materials	
Cladding	ZIRLO™
Top & Bottom Grids	Inconel 718
Middle Grids	Zircaloy-4
Guide Thimbles	Zircaloy-4
Nozzles	Stainless Steel
Holddown Springs	Inconel 718

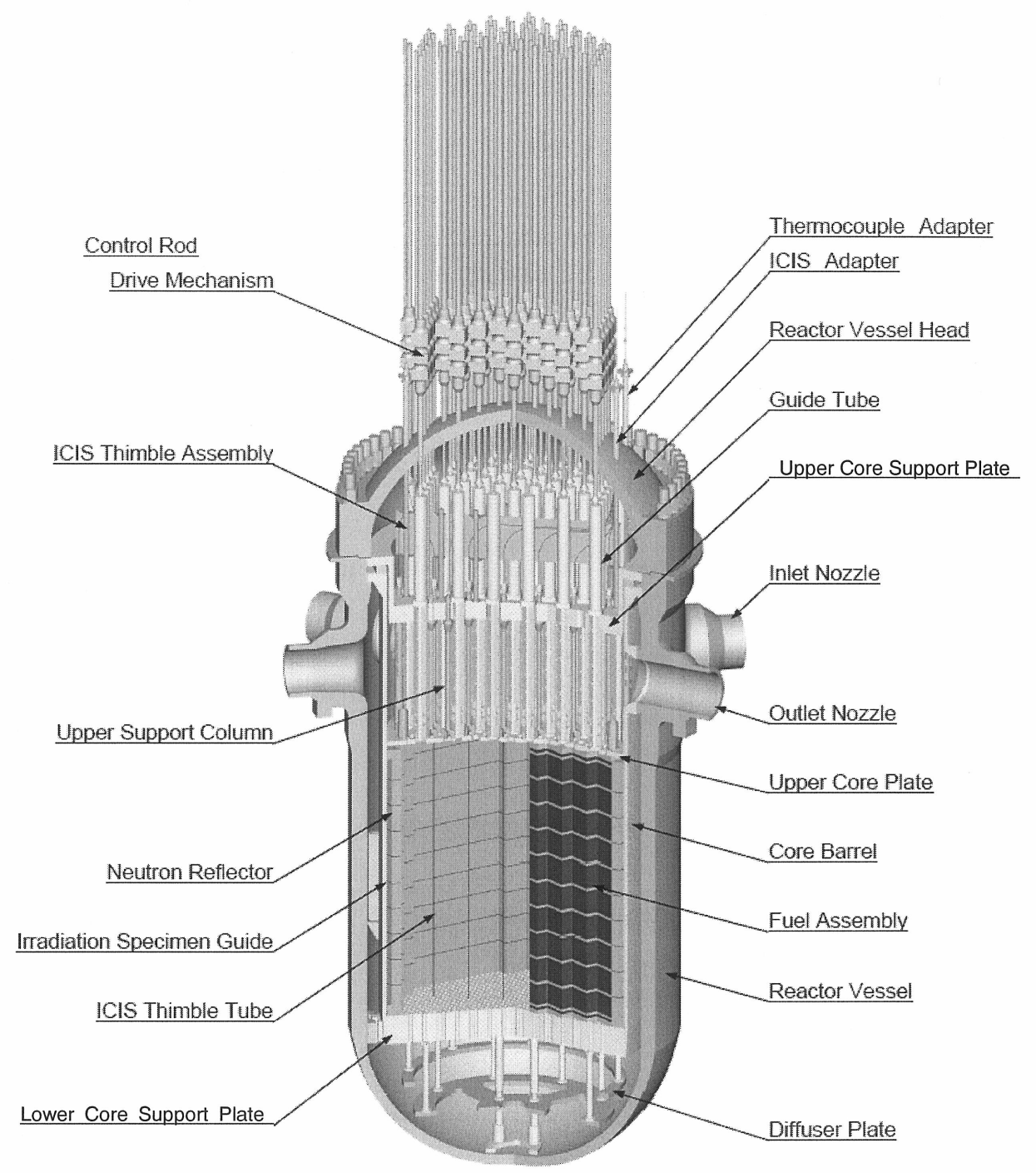

Figure 2-1 Reactor General Assembly

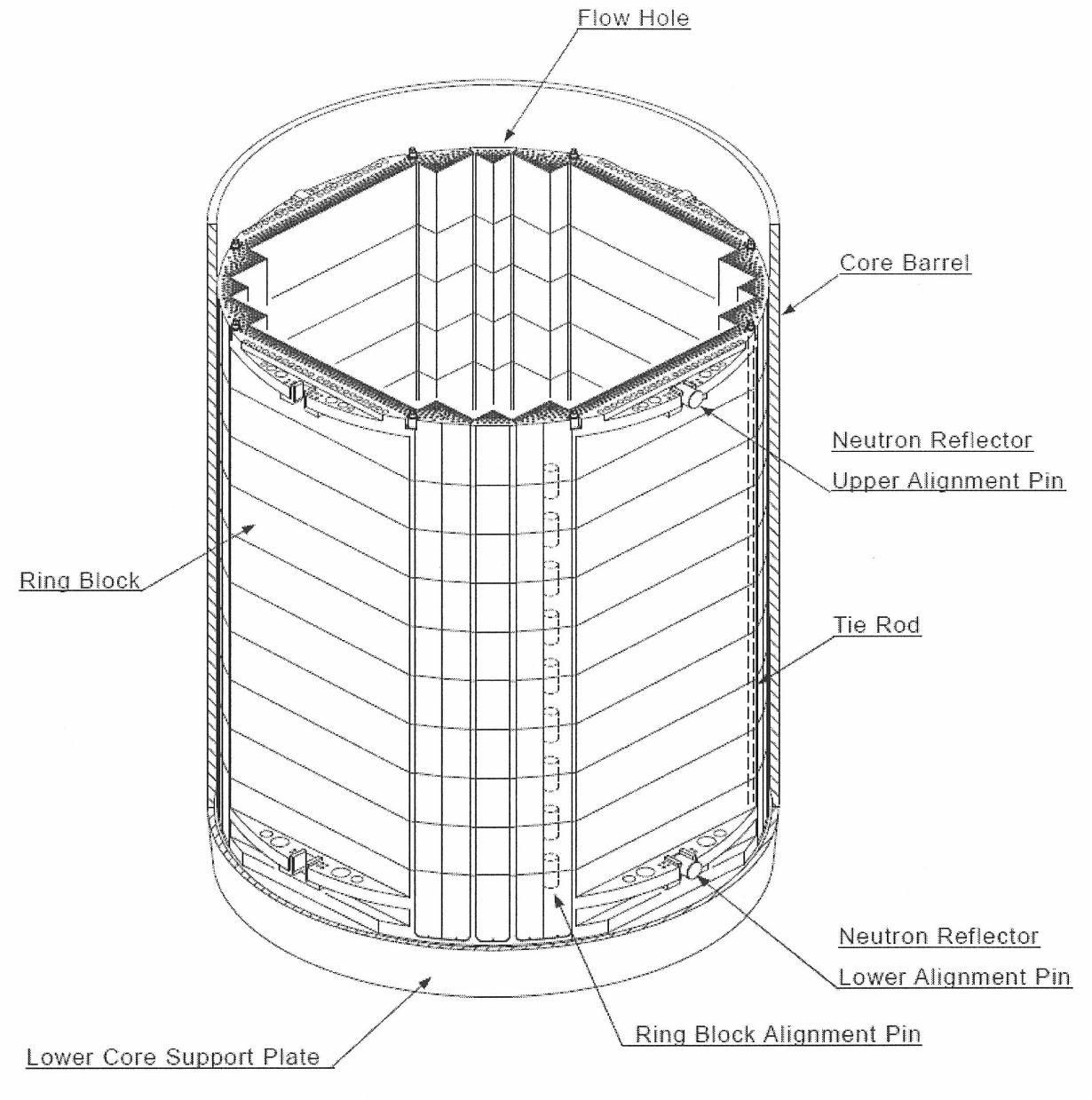

Figure 2-2 Neutron Reflector Assembly

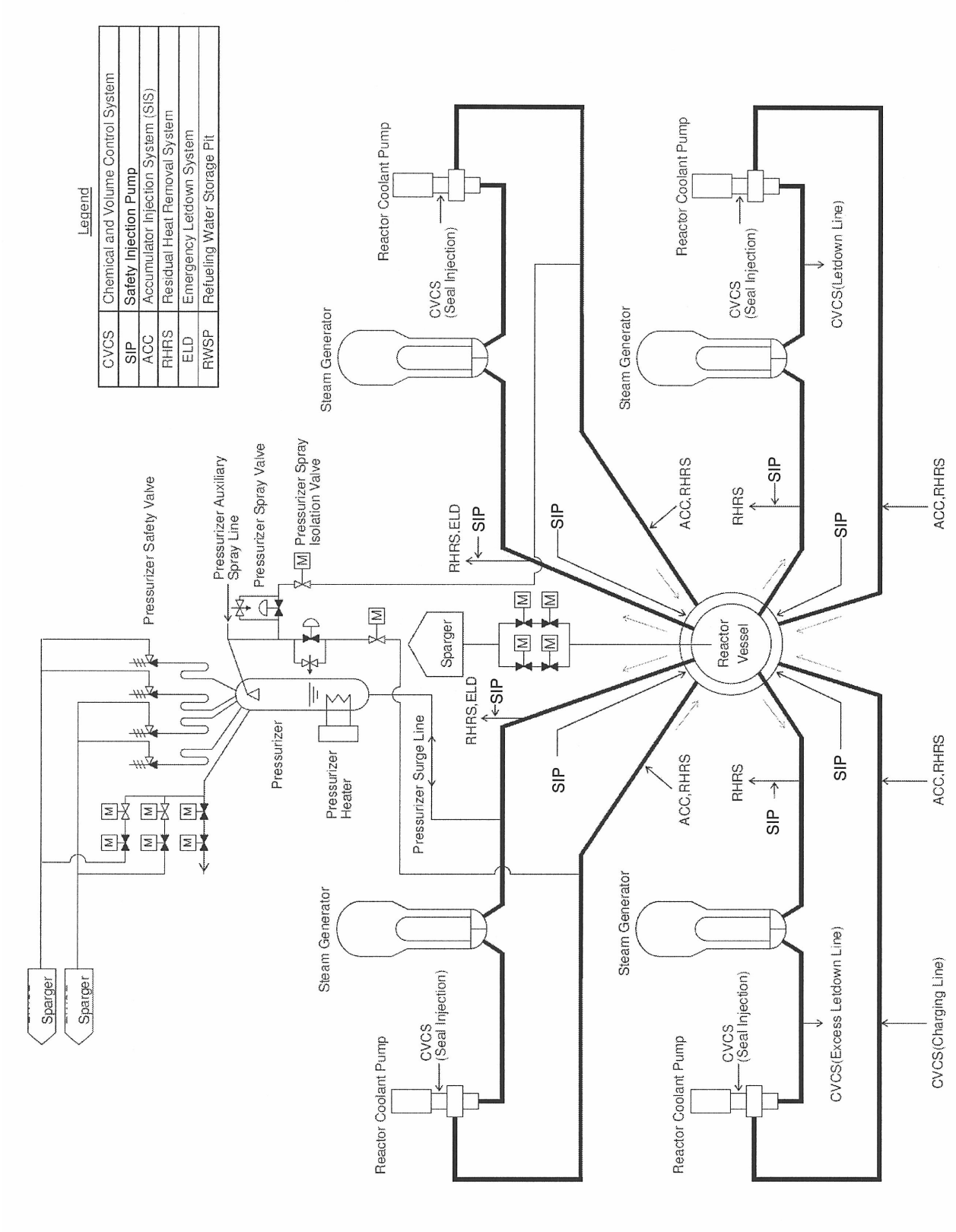

Figure 2-3 Reactor Coolant System

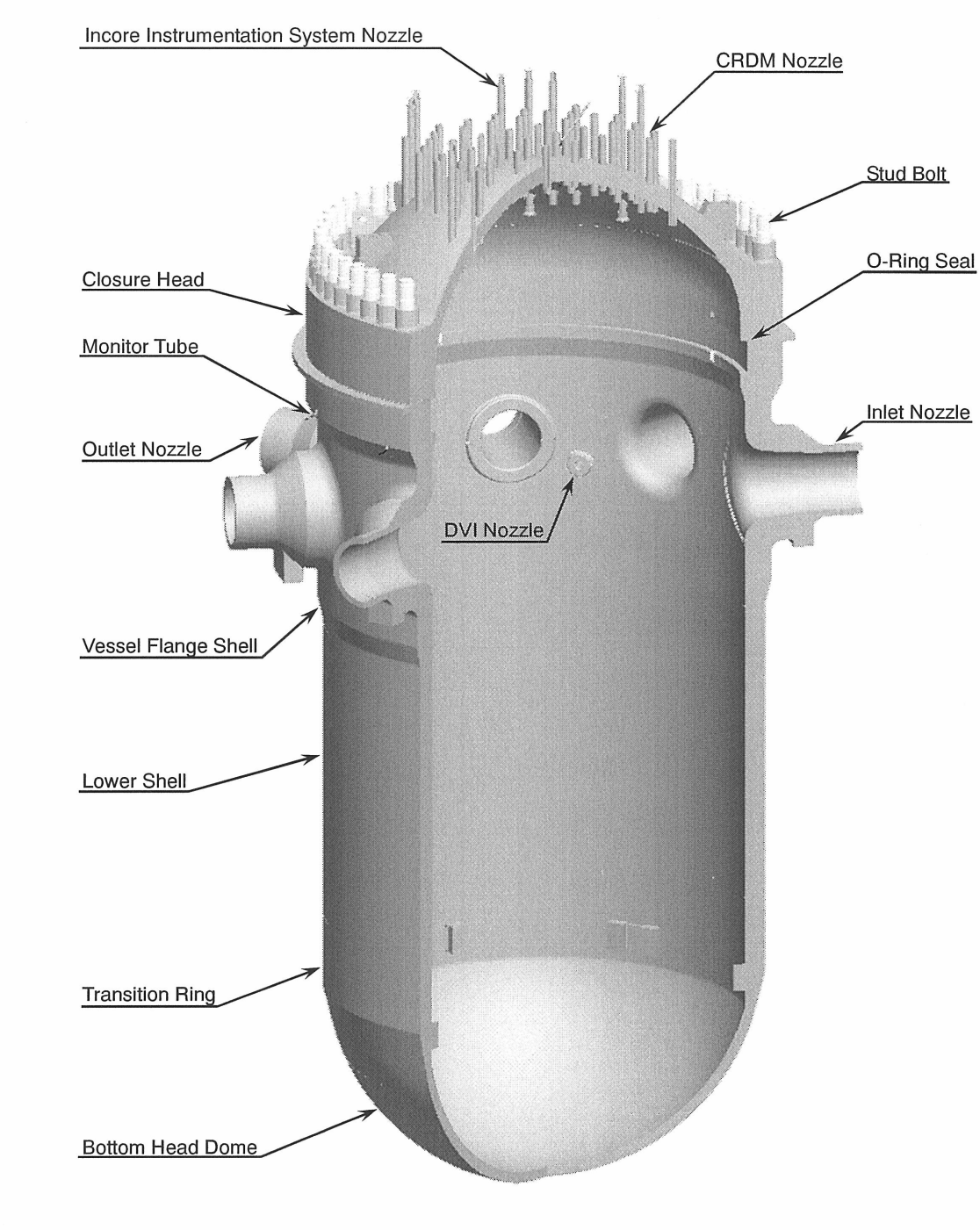

Figure 2-4 Reactor Vessel

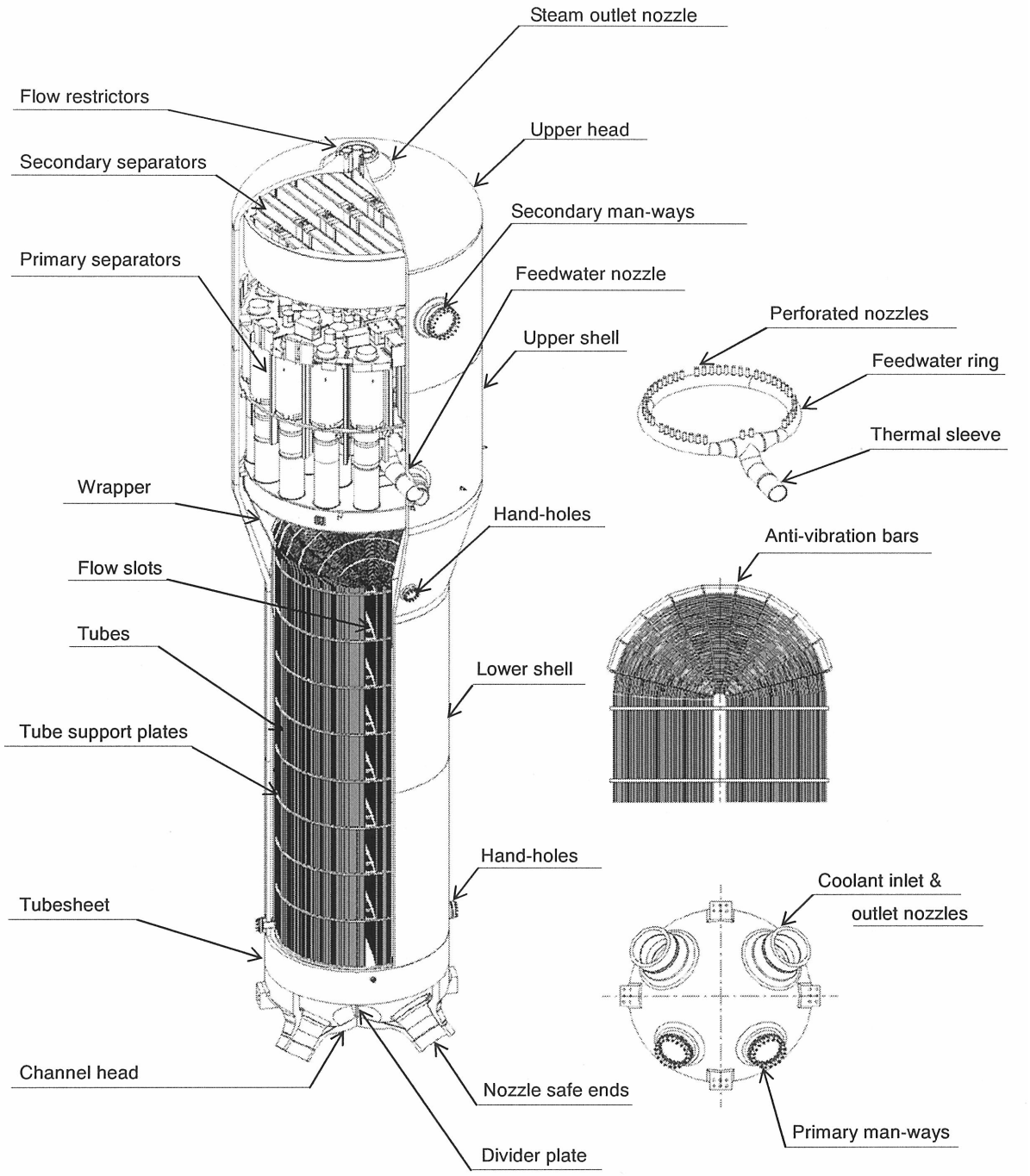

Figure 2-5 Steam Generator

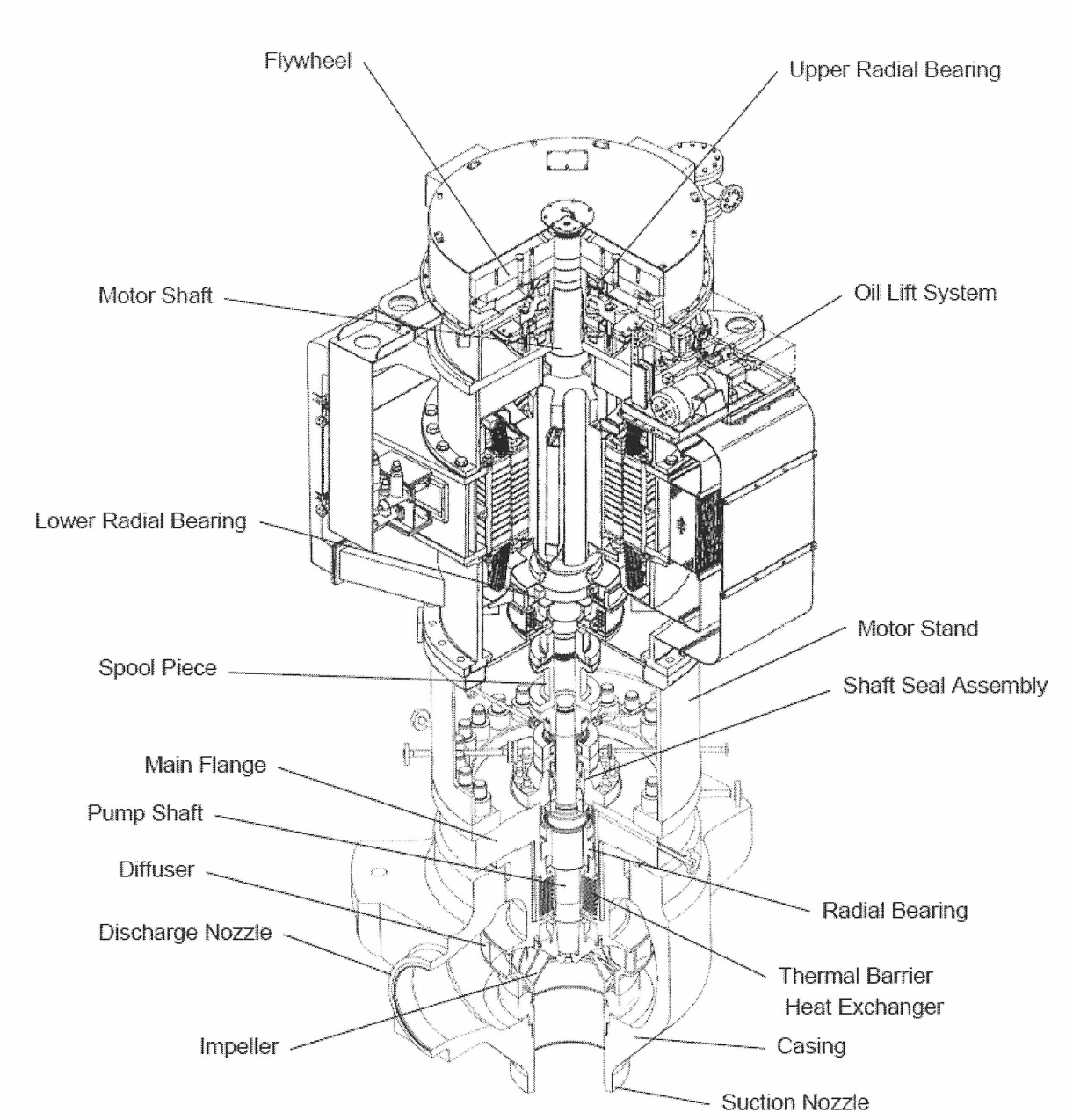

Figure 2-6 Reactor Coolant Pump

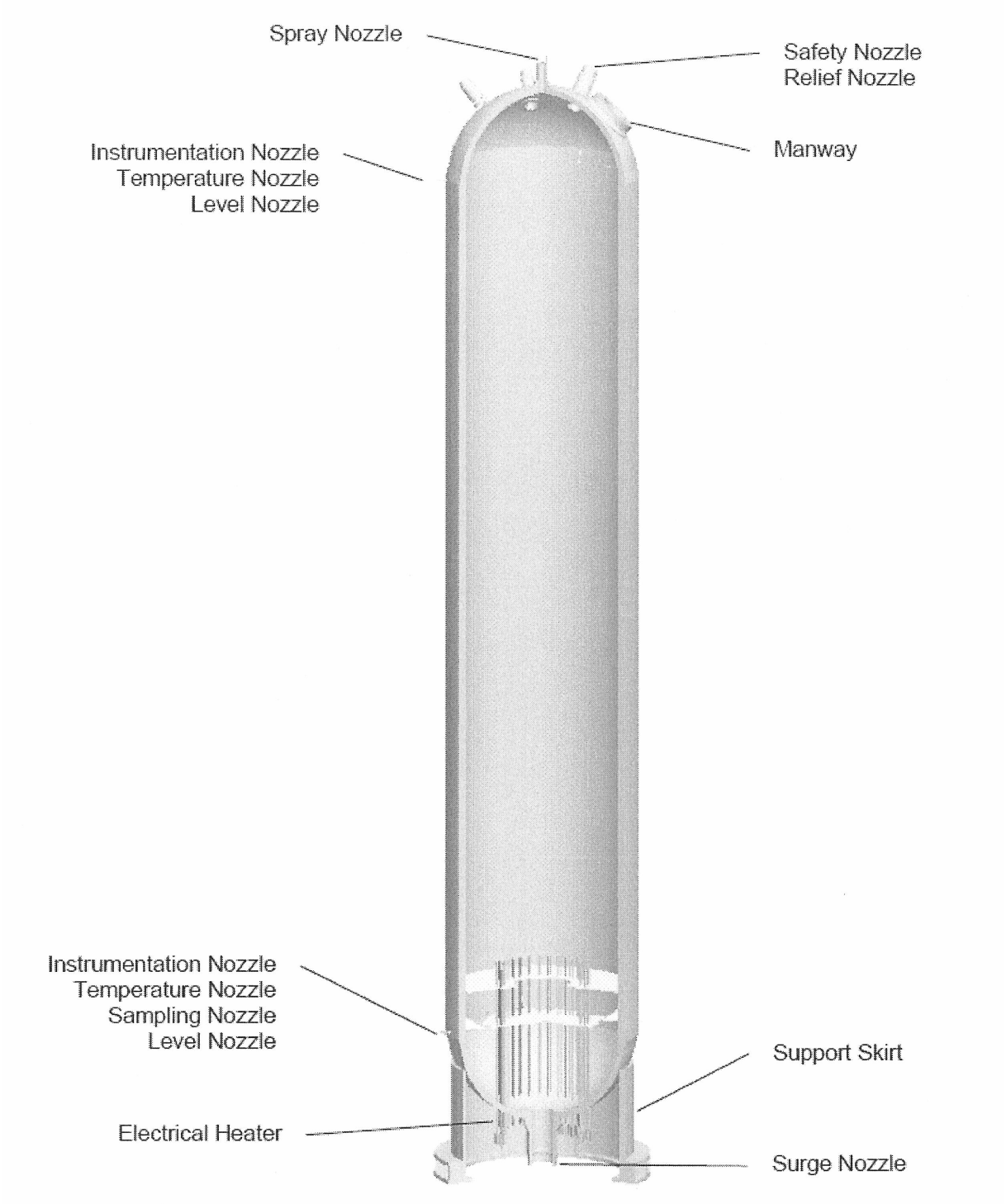

Figure 2-7 Pressurizer

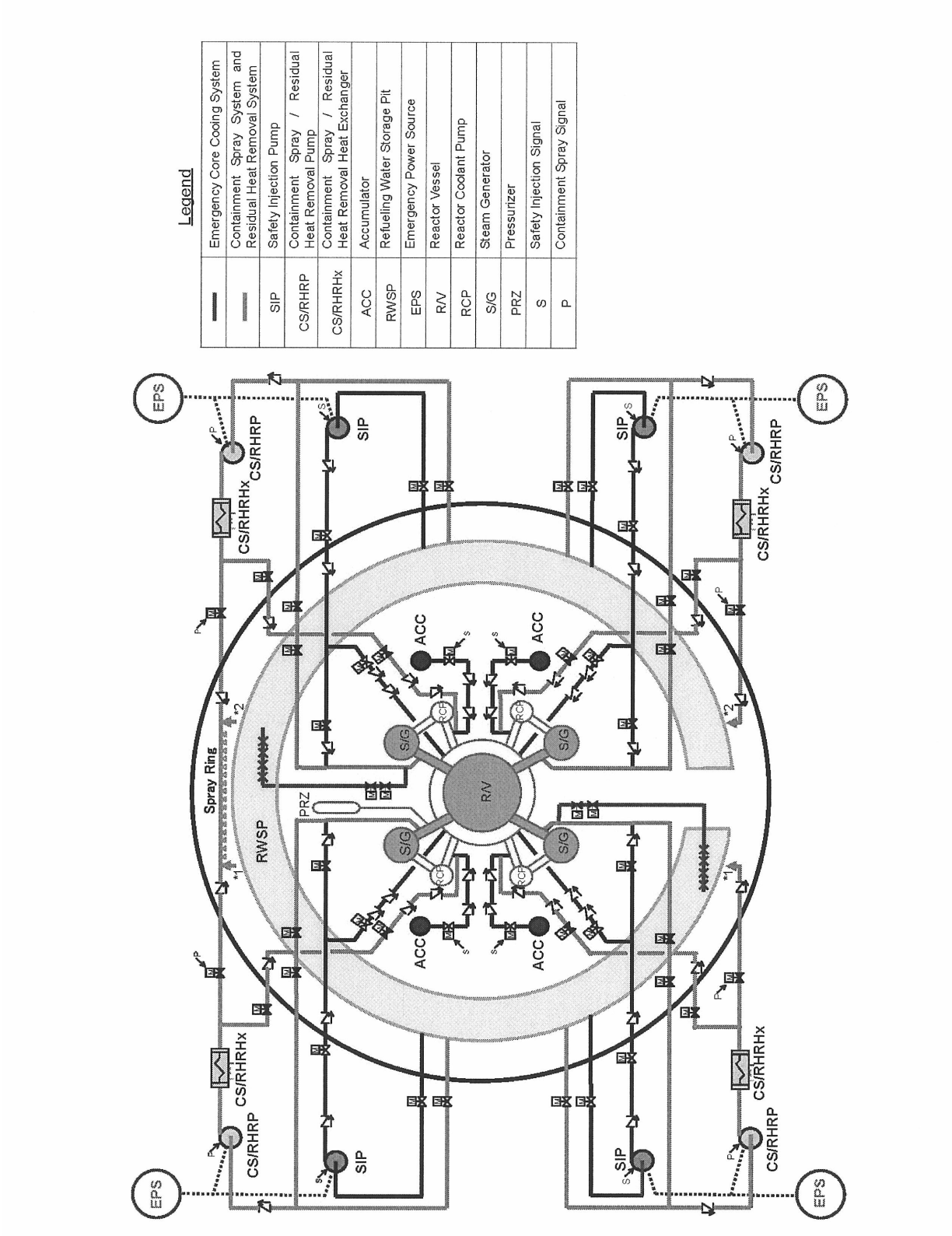

Figure 2-8 Simplified Configuration of ECCS and CSS

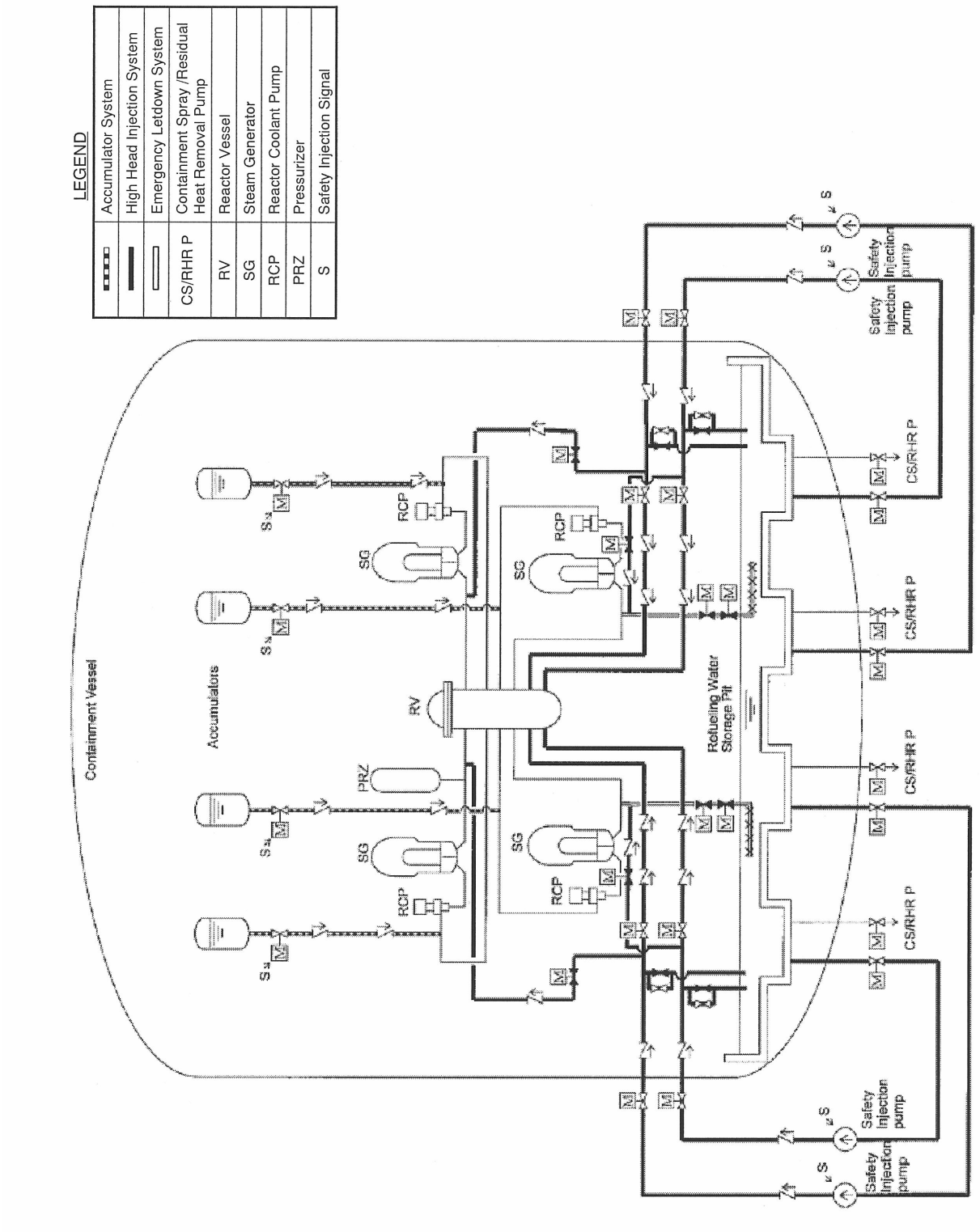

Figure 2-9 Emergency Core Cooling System

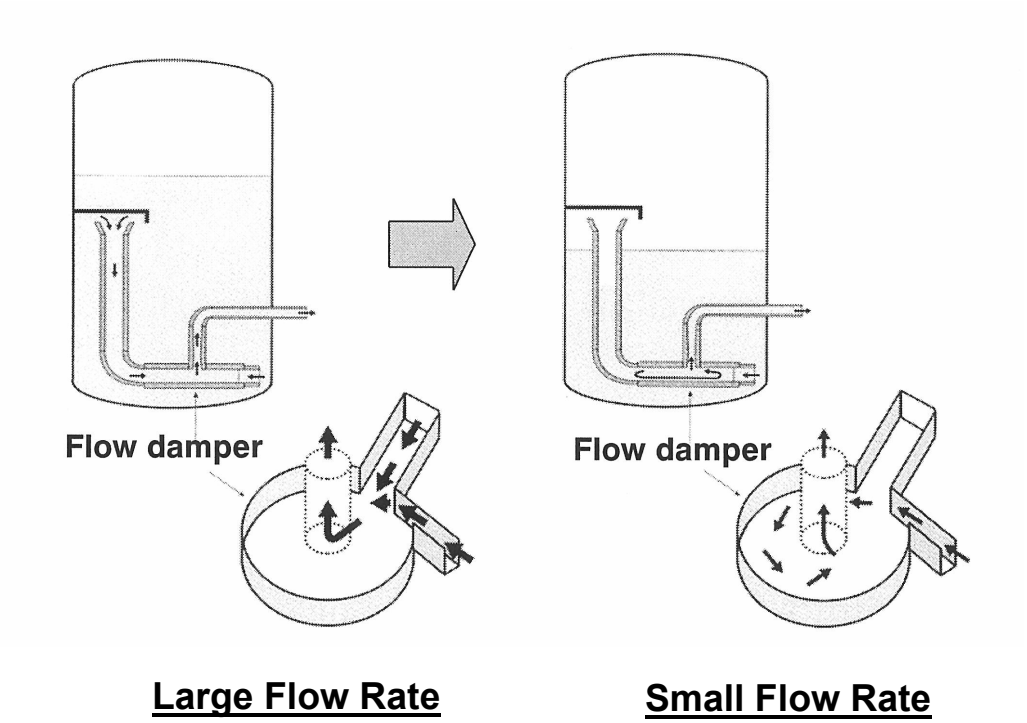

Figure 2-10 Safety System Performance for US-APWR

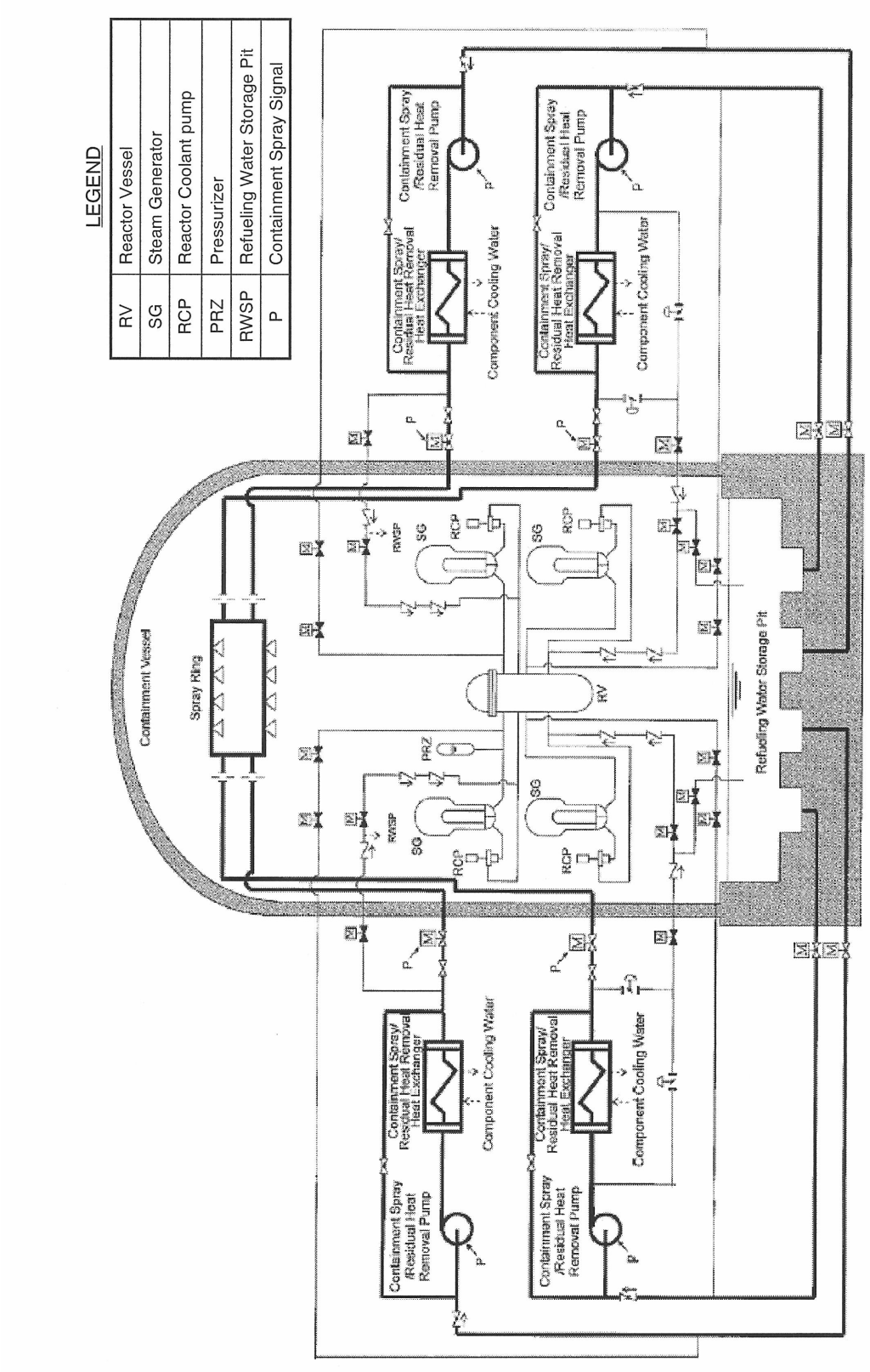

Figure 2-11 Containment Spray System

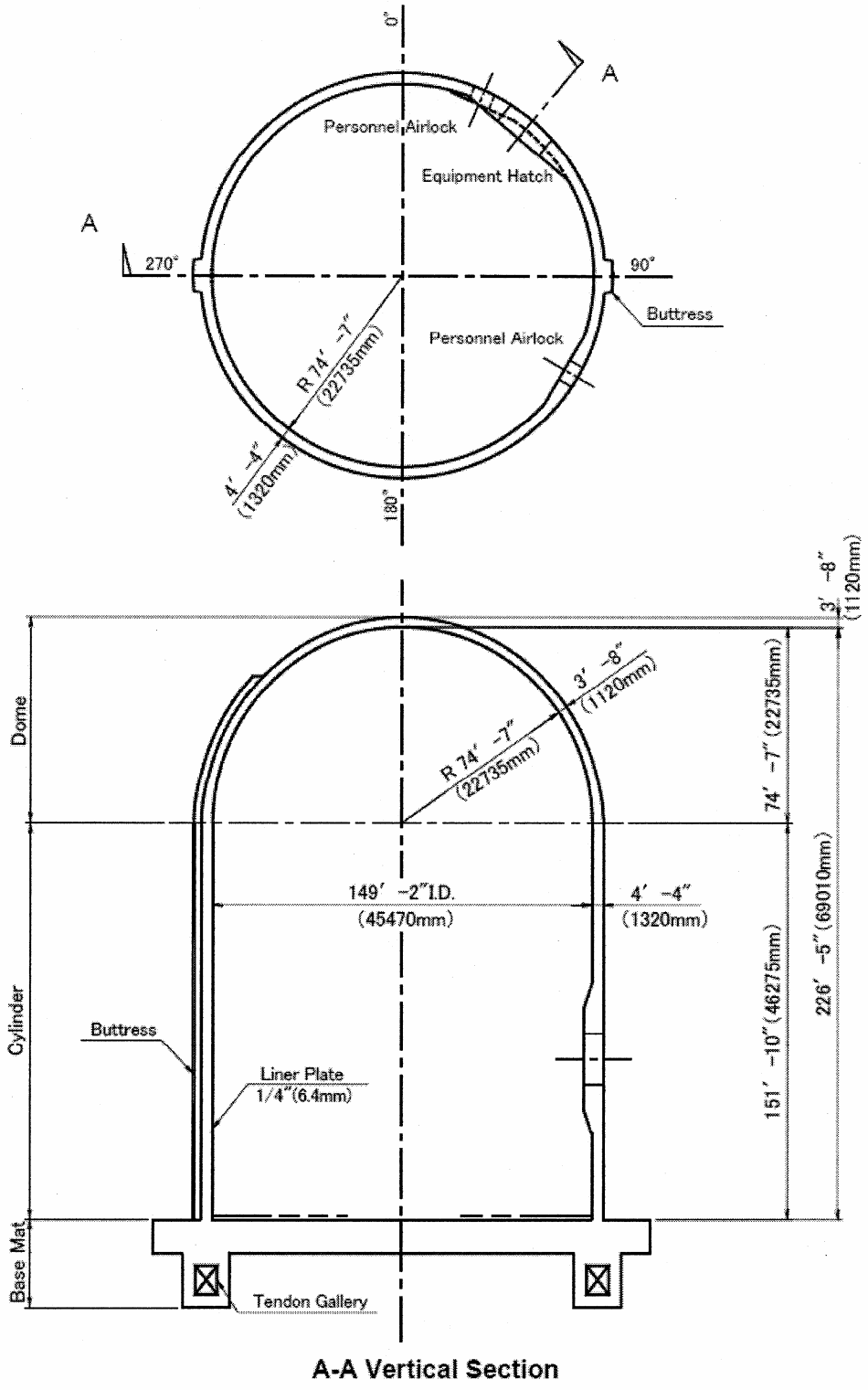

Figure 2-12 Configuration of Containment Vessel

3.0 LOCA MASS AND ENERGY RELEASE EVALUATION CODE AND METHODOLOGY

3.1 Introduction

The Standard Review Plan (Reference 1) states that LOCA mass and energy release evaluation analyses performed with the Appendix K ECCS computer codes which were developed to comply with the ECCS Acceptance Criteria presented in 10CFR50.46 and 10CFR50 Appendix K shall be acceptable. “Westinghouse LOCA Mass and Energy Release Model for Containment Design March 1979 Version (Reference 2)” conforms to the standard and is approved by the NRC.

In order to meet this standard while incorporating modified analytical models reflecting US-APWR new features, MHI has developed a modified mass and energy release model which is based on the ECCS Appendix K codes (SATAN-VI and WRFLOOD). Where applicable and appropriate, conservative models for mass and energy release calculations have been added into the codes.

The methodology for the transient mass and energy release is shown conceptually in Figure 3-1. The development of the mass and energy release calculations proceeds as follows:

1. As described in Section 3.2, the mass and energy release for the blowdown and reflood phases are calculated with SATAN-VI(M1.0) modified based on the SATAN-VI code and WREFLOOD(M1.0) modified based on the WREFLOOD code. The outputs from those codes are inputs to the GOTHIC code, which provides the transient RWSP temperature and containment back pressure in response to the calculated mass and energy release from SATAN-VI(M1.0) and WREFLOOD(M1.0).
2. The full short and long term containment response is calculated with a single GOTHIC run. The GOTHIC model includes a simplified primary/secondary system model for calculating the post-reflood mass and energy release as described in Section 3.3. During the blowdown and reflood phases, the GOTHIC primary/secondary system model is isolated and the mass and energy release from item 1 is supplied as a boundary condition for the containment. At the end of reflood, the GOTHIC primary/secondary system model is opened at the break location and the mass and energy release for the remainder of the transient is calculated by GOTHIC.

A sample containment pressure transient based on this mass and energy release model is shown in Section 3.4. A great deal of conservatism is incorporated into the MHI model, as shown in Reference 2, which specifies and quantifies the major conservatisms.

3.2 Blowdown and Reflood Phases Mass and Energy Release Evaluation Methodology

This section describes modifications to the approved Westinghouse Mass and Energy Release Model for containment design that is documented in Reference 2, and the applicability to US-APWR of these modifications for the LOCA Mass and Energy Release code and Methodology. The containment analysis code system for the blowdown and reflood phase is shown in Figure 3-1.

3.2.1 Approved Methodology

The March 1979 version of the model (Reference 2) is based on the computer codes which were developed to comply with the ECCS Acceptance Criteria presented in 10CFR50.46 and 10CFR50 Appendix K.

The following computer codes are utilized for the mass and energy release analysis during Blowdown and Reflood phases.

Blowdown	SATAN-VI	(Reference 3)
Reflood	WREFLOOD	(Reference 4)

The use of ECCS computer codes for containment mass and energy release is recognized as a valid approach by the NRC in Standard Review Plan 6.2.1.3 (Reference 1). The MHI modifications to the Westinghouse Mass and Energy Release Model are consistent with this NRC position.

The system noding scheme used for mass and energy release evaluation is the 68 node model for the SATAN-VI(M1.0) shown in Figure 3-2, which is the same as that used in the approved mass and energy release model for standard Westinghouse 2/3/4-loop plant.

A 19 element model is used to describe the system for the WREFLOOD(M1.0) code. This modeling is unchanged from that used in the approved mass and energy release model. The nodalization for the WREFLOOD(M1.0) model is shown in Figure 3-3.

3.2.2 Evaluation Approach

The US-APWR is a four-loop, pressurized-water reactor with a thermal output of 4,451 MW. Each of the four loops consists of a steam generator, reactor coolant pump, associated piping, and emergency core cooling system with the following US-APWR design features.

- Advanced Accumulator
- Direct Vessel Injection for Safety Injection Pump
- In-containment Refueling Water Storage Pit (RWSP)
- Neutron Reflector

Code modifications have been implemented to model the US-APWR design features. Also applicable range of the model for the principal parameters changed from current Westinghouse 4-loop plants has been investigated.

Section 3.2.3 provides a description and justification for the model modified during each

phase of the LOCA transient (blowdown, refill and reflood, except post reflood). It is described that the differences with the approved mass and energy release evaluation model presented in Reference 2. The use of options in the computer code input will be described along with the significant changes to the reference methodology input.

Evaluations for the modifications were made by means of comparisons with test results and/or sensitivity studies, which were selected to evaluate specific modeling modifications.

3.2.3 Code Applicability for US-APWR Features

The calculation model for LOCA analysis is divided into four phases: 1) Blowdown, which includes the period from the time of the accident inception, at steady state full power operation, to the time that the Reactor Coolant System has depressurized to the containment pressure, 2) Refill, which is the period from the end of blowdown to the time that the vessel lower plenum has been refilled by the ECCS, 3) Reflood, which begins when water enters the active core to the time that the reactor core is quenched, and 4) Post-reflood, which begins when the core is quenched and continues until the containment pressure has decreased sufficiently.

3.2.3.1 Advanced Accumulator for Blowdown, Refill and Reflood

The advanced accumulator operation has two injection modes (Reference 14). The first injection mode is basically the same as that of conventional accumulators, in which a relatively large flow is supplied. This injection mode begins during blowdown phase and continues to the early reflood phase. After the first injection mode, the second injection mode begins with a smaller injection flow rate which corresponds to injection by a conventional low head SI pump. The injection flow rate is changed by flow damper resistance, which mainly depends on the accumulator water level.

The accumulator performance model built into SATAN-VI and WREFLOOD is described below to account for its injection flow characteristics.

$$P_{gas} - P_{inj} = K_{ACC} \cdot \rho \frac{V_D^2}{2} - \rho g\left(H_t - H_p\right)$$

$$P_{gas} = \left(\frac{V_{gas0}}{V_{gas}}\right)^{\kappa} \cdot P_{gas0}$$

$$\frac{dV_{gas}}{dt} = A \cdot V_D$$

P_{gas} : Gas pressure in accumulator
P_{gas0} : Initial gas pressure in accumulator
V_{gas} : Gas volume in accumulator
V_{gas0} : Initial gas volume in accumulator
P_{inj} : Pressure at the injection point (RCS pressure)
K_{ACC} : Total resistance coefficient of the flow damper and injection piping
H_t : Difference in height between accumulator water level and vortex chamber
H_p : Difference in height between injection point and vortex chamber

V_D : Fluid velocity of the injection piping
A : Cross sectional area of the injection pipe inside
g : Acceleration of gravity
t : Time
ρ : Density of water
κ : Adiabatic exponent

In the above:
K_{ACC} has two values : $K_{ACC}=K1$ before switching of injection flow rate by flow damper.
$K_{ACC}=K2$, after switching of injection flow rate by flow damper.

The total resistance coefficient, K_{ACC}, is determined from the ACC flow rate coefficient, C_v and the resistance coefficient of the injection piping. The flow rate coefficient is a function of the cavitation factor, σ_v, and the water level in the ACC. The total resistance coefficient is calculated each time step as follows:

1) σ_v is calculated from the flow condition at flow damper

$$\sigma_v = \frac{P_D + P_{at} - P_v}{\left(P_{gas} + \rho g H_t\right) - \left(P_D + \frac{\rho V_D^2}{2} + \rho g H_D\right)}$$

σ_v : Cavitation factor
P_{at} : Atmospheric pressure
P_D : Flow damper outlet pressure (gage)
P_{gas} : Gas pressure in accumulator (gage)
P_v : Saturated vapor pressure
V_D : Fluid velocity of the injection piping
ρ : Density of water
g : Acceleration of gravity
H_t : Difference in height between accumulator water level and vortex chamber
H_D : Difference in height between flow damper outlet piping and vortex chamber

2) The flow rate coefficient C_v is calculated using the following correlations obtained from test data which cover the range of applicability for the US-APWR design

For large flow rate: $C_v = 0.7787 - 0.6889\exp\left(-0.5238\sigma_v\right)$
For small flow rate: $C_v = 0.07197 - 0.01904\exp\left(-6.818\sigma_v\right)$

3) C_v is converted to the resistance coefficient of flow damper K_D

$$K_D = 1/C_v^2$$

4) Total resistance coefficient is calculated by ;

$K_{ACC} = K_D + K_{pipe}$

K_{ACC} : Total resistance coefficient of the flow damper and injection piping
K_{pipe} : Total resistance coefficient of the injection piping

The verification of the advanced accumulator model built into the SATAN-VI and WREFLOOD codes was performed by comparing code results with hand calculations. The condition parameters of the primary loop and accumulators at various time points during accumulator operation were taken from the code output files. The code-calculated accumulator injection flow rate was compared with hand calculations by using the above equations. The result of verification is shown in Table 3-3. The flow rate obtained by the code calculation agreed with the hand calculation results.

It was therefore confirmed that the modification for SATAN-VI and WREFLOOD code was correct and that the advanced accumulator model works as expected.

The treatment of uncertainties in the accumulator initial conditions (pressure, water mass) and the injection pipe resistance will be established by sensitivity studies. For the sample analysis which is described in section 3.4, the minimum pressure, minimum water mass and maximum resistance coefficient for injection pipe were used.

3.2.3.2 Direct Vessel Injection for Reflood

The WREFLOOD code includes a steam/water mixing model which accounts for the interaction of loop steam with ECC injection water. For the ACC injection at the cold leg, a complete steam/water mixing and thermal equilibrium are assumed as in prior applications of WREFLOOD for existing PWRs.

For the pumped safety injection, there is a potential for the incomplete interaction between loop steam and safety injection flow through the DVI nozzle located at the downcomer. The degree of condensation depends on the downcomer water level and DVI nozzle location. It is conservatively assumed that there is no mixing of steam and safety injection water through the DVI nozzles to maximize the energy release to the containment. This is conceptually shown in Figure 3-4.

To verify the assumption for condensation on the pumped safety injection flow, sensitivity studies were performed to evaluate the impact of the mixing assumption for the DVI in the US-APWR containment mass and energy release analyses. Both cases are calculated until end of reflood phase.

Case 1 : No steam/water mixing at DVI point
Case 2 : complete steam/water mixing at DVI point
(note: Complete steam/water mixing at ACC injection point was assumed in both cases. Other assumptions, initial conditions, etc. are identical for the two cases.)

The results of the sensitivity studies are shown in Figure 3-5 and Figure 3-6 with results from both cases. Figure 3-5 shows that the integral of energy flow rate from the break for case 1 (No steam/water mixing at DVI point) rises faster than that of case 2 (complete steam/water mixing at DVI point). The containment internal pressure for case 1 is slightly higher than that of case 2 (Figure 3-6). Therefore case 1 is assumed in the mass and energy release analysis

to provide conservative results for containment integrity evaluation.

3.2.3.3 Refueling Water Storage Pit (RWSP) for Reflood

In the US-APWR design, the RWSP is located at the bottom periphery of the containment and connected to the containment atmosphere with pipes. Hence liquid and steam released from the RCS flow into the RWSP and the RWSP water temperature changes during LOCA transients. As the RWSP temperature changes, the safety injection water temperature will also change continuously. The containment back pressure as RWSP back pressure also will change as the transient progresses. The reflood and flow rate of safety injection is affected by containment back pressure.

For the currently approved mass and energy release evaluation methodology, the safety injection water temperature was constant because the RWSP is outside the containment. Also high containment back pressure (design pressure) was assumed. For the US-APWR design the RWSP is located within the containment. Therefore, it is necessary to couple mass and energy release calculation to containment response to model the changing RWSP water temperature and containment back pressure.

To achieve the above modeling, the WREFLOOD(M1.0) code was synchronized with the containment response analysis code (GOTHIC) to compute RWSP water enthalpy and containment back pressure at each time step. A modification to allow this code coupling was needed only for the WREFLOOD code. The original GOTHIC code has built-in capabilities (referred to as Inter Process Communications) to send or receive data with external codes, so there was no modification of necessity for GOTHIC.

These modifications for the WREFLOOD code affect only the input data handling and do not change the analytical method.

3.2.3.4 Neutron Reflector for Reflood

Figure 3-7 shows the NR. The NR consists of ten thick stainless steel blocks and is heated by gamma irradiation during normal operation. The NR is designed to be cooled by up flow through the cooling holes in the blocks to prevent excessive stress and thermal deflections of the blocks due to the gamma heating. As a result of the cooling that is provided, the temperature of the neutron reflector is kept around average fluid temperature during normal operation.

In a postulated loss-of-coolant accident (LOCA), the NR works as a heat source to the containment similar to other metal in the primary system. During the blowdown phase a small part of the stored energy is released as the fluid temperature decreases. During the reflood phase the NR has experiences quenching like does the core due to the NR’s large mass and the large heat transfer area.

The steam generation due to cooling of the NR increases the energy release rate to the containment. Similarly, entrainment of liquid from the NR into the upper plenum and the steam generator increases the heat release rate from the secondary side of the steam generator to the containment. These two effects would also reduce the flooding rate. Therefore the NR is expected to cause longer reflood period with a little larger energy

release rate, which results in small increase of the containment pressure. The effect, however, is considered to be quantitatively small because the stored energy of the NR is only about 〔 〕% of the energy released from the core during reflood period.

〔

〕

Validity of the above modeling approach for a conservative analysis was confirmed by the simulation of phenomena related to the NR during the reflood phase with the best-estimate code, WCOBRA/TRAC. The results of the study are described in Appendix C.

3.2.3.5 Parameter Range

Since the US-APWR has design, geometric, functional, and phenomenological similarities to current Westinghouse 4-loop PWRs, the model approved for them can be basically applied to the US-APWR with modifications concerning its specific features.

This section describes whether applicable range of physical models in the codes covers the range of parameters during LOCA for the US-APWR.

As shown in Table 2-1 the US-APWR has the following characteristics compared with current 4-loop PWRs.

- Almost same operating fluid conditions
- Lower average linear heat rate by increasing fuel length
- Higher containment design pressure

As to the blowdown analysis, since the constitutive models of the SATAN-VI code are generic and cover wide range of parameters from the normal operation to the end of blowdown when the primary system pressure settles close to the containment pressure, the above two difference will not affect applicable range of the code.

However, the WREFLOOD code used for the reflood phase has the specific correlation for reflooding of the core. That is the correlation for the mass effluent fraction as shown below.

Where:

F_{out} = Fraction of inlet water not stored below the quench front and assumed to exit core.

Z_q = Quench front level in core, inch.

$Q'\max$ = Peak heat generation rate, kW/ft. (*1)

P = System pressure, psia.

ΔT_{sub} = Inlet water subcooling, $^\circ F$.

V_{in} = Inlet water flooding rate, inch/sec.

(*1)

As the reflood water enters the bottom region of the core during the reflood transient and comes into contact with hot fuel rods, boiling occurs in the core. The steam thus formed in the lower region of the core flows up through the core and vented through the reactor coolant loops. As the steam flows up through the core, part of the reflood water in the core is entrained in the steam and carried out of the vessel. To account for the steam flow with entrained water from the core to the loops, above empirical correlation was developed from FLECHT (Reference 16) experimental results.

This correlation was validated as shown in Figure 3-8 and Figure 3-9, which are from Reference 4, and has been used for Westinghouse-type PWRs.

As described before the US-APWR has lower average linear heat rate and higher containment design pressure, which results in higher system pressure during reflood phase, compared with current 4-loop plants.

The peak heat generation rate, $Q'\max$ in the correlation is calculated using average linear heat rate, decay heat fraction at the beginning of the reflood and peaking factor based on FLECHT tests, which is around 0.5kW/ft for a typical current 4-loop plant with 12-ft core.

[redacted]

As described above $Q'_{\max}$ of a typical current 4-loop plant is around 0.5kW/ft. However, this is not necessarily within the range of validation, 0.69 through 1.24 kW/ft, as shown in the table on Figure 3-8, where peak heat generation rate is called peak power. In order to confirm performance of the correlation, comparison with the FLECHT SEASET (Reference 17) data with lower peak heat generation rate was performed.

FLECHT SEASET program was conducted using rod bundle simulating 17x17 type fuel assembly to provide data and analysis that would improve understanding of the complex two-phase flow phenomena that occurs during a postulated PWR loss-of-coolant accident.

The following test data, which show effects of peak power, were selected from Unblocked Bundle Reflood Task series, the initial phase in the comprehensive tasks of the FLECHT SEASET program. Other conditions of the tests except peak power are within the range of Fout correlation.

Run number	31203	31021	34524
Pressure	40 psia	40 psia	40 psia
Peak power	0.7 kW/ft	0.4kW/ft	1.0kW/ft
Flooding rate	1.51 inch/sec	1.52 inch/sec	1.57inch/sec
Subcooling	141 F	141F	142F

[redacted]

Figure 3-10 compares carryout fraction by the correlation with test data. The calculation was performed by spreadsheet software. The carryout fraction is defined as the next expression.

$$Carryout\ Fraction = \frac{Mass\ out(lbm)}{Mass\ in(lbm)}$$

Excellent agreement with data is noted in the low power region, which proves that the correlation is applicable to 17x17 type fuels with lower linear power.

3.3 Post-reflood Mass and Energy Release Evaluation Methodology

The post-reflood mass and energy release analysis is performed with the GOTHIC computer code (Reference 5). The MHI's approach allows the mass and energy release from the primary system to be coupled with the containment response calculation because both are included in the same model. The US-APWR mass and energy release model is similar to the model used by Dominion in their containment analysis methodology, which was previously approved by the NRC (Reference 8) for Surry. In the Surry application (Reference 2), it was shown that the methodology described here gave a post-reflood mass and energy release rate that closely matched the previously approved Westinghouse methodology (Reference 8).

The details of the post-reflood mass and energy release along with an overview of the GOTHIC code are provided below.

3.3.1 GOTHIC Computer Code Overview

GOTHIC is a general purpose thermal-hydraulics code for performing design, licensing, safety and operating analysis of nuclear power plant containments and other confinement buildings. GOTHIC was developed for the Electric Power Research Institute (EPRI) by Numerical Applications, Inc. (NAI) (Reference 5). A summary description of GOTHIC capabilities is given below. More detailed descriptions of the code user options, models and qualification are documented in References (5,6,7).

GOTHIC solves the conservation equations for mass, momentum and energy for multicomponent, multi-phase flow in lumped parameter and/or multi-dimensional geometries. The phase balance equations are coupled by mechanistic models for interface mass, energy and momentum transfer that cover the entire flow regime from bubbly flow to film/drop flow, as well as single phase flows. The interface models allow for the possibility of thermal non equilibrium between phases and unequal phase velocities, including countercurrent flow. GOTHIC includes full treatment of the momentum transport terms in multi-dimensional models, with optional models for turbulent shear and turbulent mass and energy diffusion. Other phenomena include models for commonly available safety equipment, heat transfer to structures, hydrogen burn and isotope transport.

Conservation equations are solved for up to three primary fields and three secondary fields. The primary fields are steam/gas mixture, continuous liquid and liquid droplet; the secondary fields are mist, ice, and liquid components. For the primary fields, GOTHIC calculates the relative velocities between the separate but interacting fluid fields, including the effects of two-phase slip on pressure drop. GOTHIC also calculates heat transfer between phases, and between surfaces and the fluid. Reduced equation sets are solved for the secondary fields by the application of appropriate assumptions as described in the reference documents.

The three primary fluid fields may be in thermal non equilibrium in the same computational cell. For example, saturated steam may exist in the presence of a superheated pool and subcooled drops. The solver can model a wide range of fluid conditions that encompass the expected containment and primary/secondary system conditions for the US-APWR LOCA analysis.

The steam/gas mixture is referred to as the vapor phase and is comprised of steam and, optionally, up to eight different noncondensing gases. The noncondensing gases available in

the model are defined by the user. Mass balances are solved for each component of the steam/gas mixture, thereby providing the volume fraction of each type of gas in the mixture.

The mist field is included to track very small water droplets that form when the containment atmosphere becomes super saturated with steam. The liquid component field allows particles or liquid globules to be tracked in the liquid phase. The ice field models melting, freezing, and sublimation and is used for ice condenser containment modeling.

The principal element of the model is a control volume, which is used to model the space within a building or subsystem that is occupied by fluid. The fluid may include noncondensing gases, steam, drops or liquid water. GOTHIC features a flexible noding scheme that allows computational volumes to be treated as lumped parameter (single node) or one-, two- or three-dimensional, or any combination of these within a single model.

Solid structures are referred to in GOTHIC as thermal conductors. Thermal conductors are modeled as one-dimensional slabs for which heat transfer occurs between the fluid and the conductor surfaces and, within a conductor, perpendicular to the surfaces. The one-dimensional thermal conductors can be combined into a conductor assembly to model two-dimensional conduction.

GOTHIC includes a general model for heat transfer between thermal conductors and the steam/gas mixture or the liquid. There is no direct heat transfer between thermal conductors and liquid droplets. Thermal conductors can exchange heat by thermal radiation. Any number of conductors can be assigned to a volume.

Fluid boundary conditions allow the user to specify mass sources and sinks and energy sources and sinks for control volumes. Thermal boundary conditions applied through a heat transfer option on a thermal conductor surface can be used as energy sources and sinks for solid structures.

There are four features in GOTHIC for modeling hydraulic connections. These are flow paths, network models, cell interface connections in subdivided volumes, and 3D connectors for subdivided volumes. Flow paths model hydraulic connections between any two computational cells, which includes lumped parameter volumes and cells in subdivided volumes. Flow paths are also used to connect boundary conditions to computational cells where mass, momentum and energy can be added or removed. A separate set of momentum equations is solved for flow paths.

Network nodes and links are available specifically for modeling building ventilation or piping systems. These types of hydraulic connections can include multiple branches between connected volumes. Network nodes are assigned to the branch points.

Adjacent cells within a subdivided volume communicate across the cell interface, based on the characteristics of the hydraulic connection. 3D flow connectors define the hydraulic connection across cell interfaces that are common to two subdivided volumes.

GOTHIC includes an extensive set of models for operating equipment. These items include pumps and fans, valves and doors, heat exchangers and fan coolers, vacuum breakers, spray nozzles, coolers and heaters, volumetric fans, hydrogen recombiners, ignitors, pressure relief valves.

Initial conditions allow the user to specify the state of the fluid and solid structures within the modeled region at the start of a transient. These include the initial temperature and composition of the containment atmosphere, the location and temperature of liquid pools, the location and amount of liquid components, and the temperatures of solid structures within the building.

Additional resources available to expand the realm of situations that can be modeled by GOTHIC include functions, control variables, trips and material properties.

3.3.2 Modeling Approach

The approach for the post-reflood mass and energy release analysis utilizes an integrated GOTHIC model that calculates both the primary system post reflood behavior following a LOCA and the corresponding containment response. During a LOCA event, most of the vessel water will be displaced by the steam generated by flashing. The vessel is then refilled by the advanced accumulators and high head injection systems. GOTHIC is not suitable for modeling the reflood period because it involves quenching of the fuel rods where film boiling conditions may exist. Current versions of GOTHIC do not have models for quenching and film boiling. For the period from LOCA initiation through the end of reflood, the mass and energy release rates are obtained from the SATAN-VI(M1.0) and WREFLOOD(M1.0) codes, as described in the Section 3.2, and supplied to the GOTHIC containment model through boundary conditions.

GOTHIC can model the primary system mass and energy release after the core has been recovered. Beyond this time, injection systems continue to supply water to the vessel. Residual stored energy and decay heat comes from the fuel rods. Stored energy in the vessel and primary system metal are also gradually released to the injection water which eventually spills out the break and into the containment.

Buoyancy driven circulation through the intact steam generator loops will remove stored energy from the steam generator metal and the water on the secondary side. Depending on the location of the break, the water injected into the primary system may pass through the steam generator on the broken loop and pick up heat from the stored energy in the secondary system.

The post-reflood mass and energy release must account for the transfer of decay heat and the stored energy in the primary and secondary systems to the containment. The following paragraphs describe the methodology used to analyze these phenomena in GOTHIC. Key elements of the containment model are summarized first, followed by a description of the primary system model.

3.3.2.1 GOTHIC Containment Model

Since the GOTHIC containment model is an integral part of the mass and energy release calculation through its coupling with SATAN-VI(M1.0) and WREFLOOD(M1.0) and post-reflood mass and energy discussed here, the GOTHIC containment model is briefly described here.

Consistent with approved methods for existing PWR LOCA containment response, the US-APWR containment is modeled [ ]. The RWSP is included as a pool at

the bottom of the containment. [

]

The model includes passive heat sinks for the containment shell and interior concrete and metal. The convective and condensation heat transfer is modeled using NRC approved methods.

The break flow is modeled by liquid, drop and steam injection as appropriate for the primary system conditions in a manner that is consistent with previously approved methods.

The containment sprays are modeled using the GOTHIC drop field. The water is taken from the RWSP, passed through the CS heat exchanger and injected at the nozzle manufacturer's specified nominal drop size. GOTHIC's interfacial heat and mass transfer models are used to calculate the effectiveness of the containment sprays.

3.3.2.2 GOTHIC Mass and Energy Release Analysis Methodology

GOTHIC is used to model the primary system mass and energy release after the core has been quenched. The modeling approach described below is similar to that used in previous analyses that have been reviewed and approved by the NRC (Reference 8).

Noding
The GOTHIC noding for US-APWR post-reflood mass and energy release analysis is shown in Figure 3-11 and Table 3-4 describes each node. [

]

(

)

In order to calculate the natural circulation through the intact loop and the correct water level in the vessel and downcomer, accurate bottom elevations and heights are specified for all of the primary system volumes.

(

)

Conductors

Conductors are included to model the stored energy in the primary system and the steam generators and to model the heat transfer across the steam generator tube surfaces. The initial temperatures for the conductors are set such that the remaining stored energy at the end of reflood, as calculated by WREFLOOD(M1.0) is conserved.

Core decay heat is modeled using a heater component with a time dependent heat rate. The ANS 1979 decay heat curve with two sigma uncertainty (Reference 11,12,13) is modeled . The decay heat is assumed to be based on infinite time at full power. The decay heat curve used in the GOTHIC modeling is consistent with the reflood phase analysis.

Vessel Froth Level

During the early part of the post-reflood phase, there is substantial boiling in the vessel due to the decay heat and the release of stored energy in the fuel, vessel and internals. The boiling raises the surface level of the water in the vessel. The surface level affects the amount of water that is carried into the steam generators with the steam produced in the vessel and, consequently, the rate of energy removal from the steam generators. The stored energy in the steam generators will be released more quickly if there is significant water carried into the steam generators.

Steam Condensation in Cold Leg and Downcomer Volumes

In the US-APWR design, cold water from the accumulators is injected into the cold leg, while safety injection water from the RWSP is introduced directly into the downcomer. The mixing of the cold injected water with steam from the steam generators influences the condensation rate, the flow rate through the steam generators and the steam flow to the containment.

Experimental evidence (Reference 10) indicates that during safety injection in the post-reflood phase, the cold leg condensation rate is maximized. These tests were for a 1/3 scale (10” diameter) cold leg.

This approach is consistent with the experimental evidence and with previously accepted methods for treating the cold leg injection (Reference 8).

In the downcomer volume, the model liquid/vapor interface area is set to zero. Therefore the condensation in the downcomer due to the direct vessel injection is not considered. This is the conservative assumption to obtain higher containment pressure and temperature.

3.4 Sample Analysis for US-APWR

A sample analysis for US-APWR was performed by using the codes described above; SATAN-VI(M1.0), WREFLOOD(M1.0) and GOTHIC(*1). The main parameters used in mass and energy release and containment response analysis are shown in Table 3-5. A double ended guillotine break at pump suction was assumed as postulated LOCA condition.

The mass and energy release results of each phase are shown Figure 3-12 to Figure 3-17, and containment pressure and vapor temperature are shown in Figure 3-18 and Figure 3-19. The peak pressure is 57.5 psig which appears at 1964 sec. The peak temperature of the vapor is 282 deg F at 1797 sec.

(*1) The GOTHIC code version used in the sample analysis is “GOTHIC 7.2a-p5(QA)”.

Table 3-1 SATAN-VI Code Noding for Blowdown Phase Mass & Energy Release Analysis

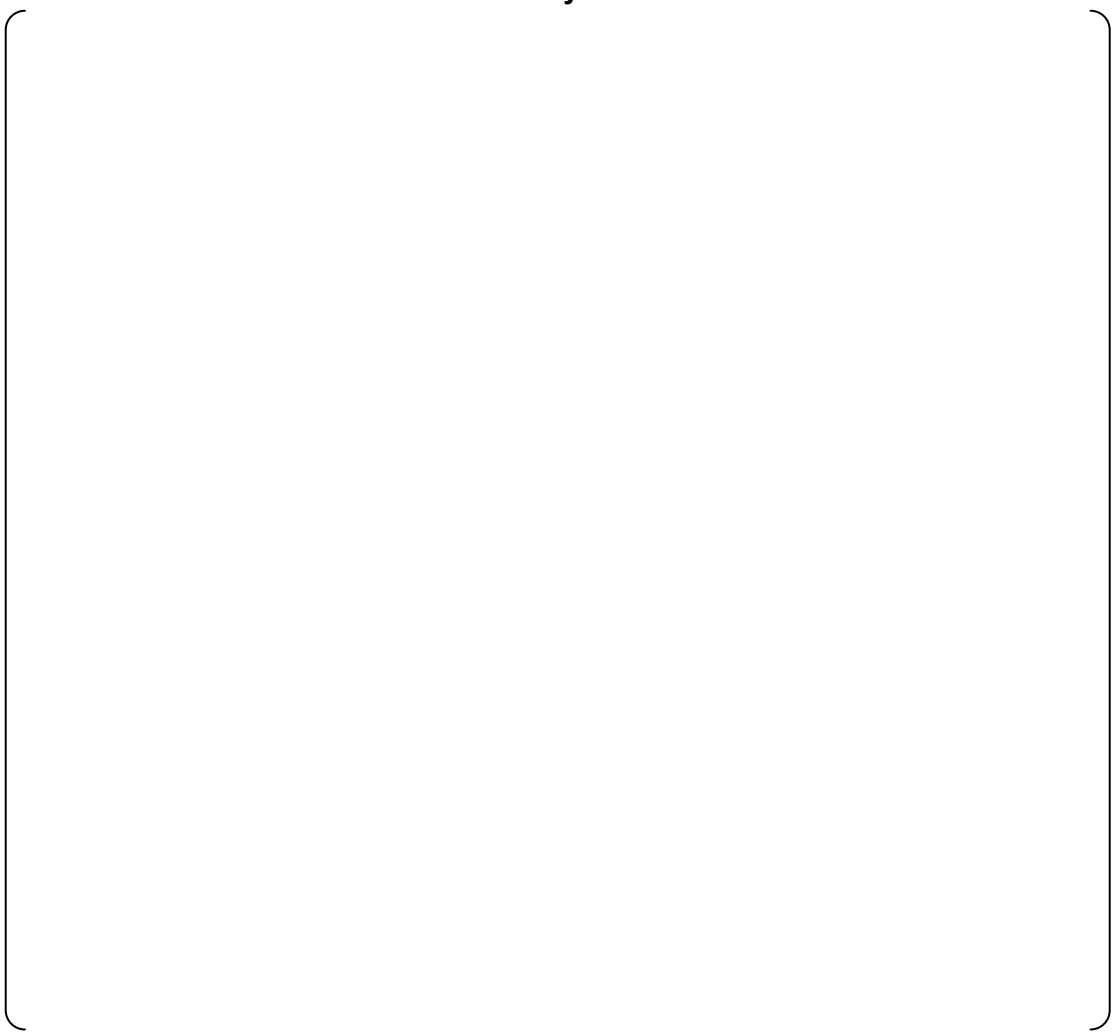

Table 3-2 WREFLOOD Code Noding for Reflood Phase Mass and Energy Release Analysis

Node	Physical description
Loop 1 (broken loop)	
1	Outlet nozzle of reactor vessel
2	Hot leg
3	SG inlet plenum
4	SG tubes
5	SG outlet plenum
6	Pump suction leg
Loop 2 (Intact loop)	
1	Outlet nozzle of reactor vessel
2	Hot leg
3	SG inlet plenum
4	SG tubes
5	SG outlet plenum
6	Pump suction leg
7	Reactor coolant pump
8	Cold leg
9	Inlet nozzle of reactor vessel
10	Downcomer
11	Inlet nozzle of reactor vessel
12	Cold leg
13	Reactor coolant pump

Table 3-3 Verification of Advanced Accumulator Model Built into SATAN-VI and WREFLOOD Code

Table 3-4 GOTHIC Code Noding for Post-reflood Mass and Energy Release Analysis

Table 3-5 Main Input Description for Sample Analysis of Mass and Energy Release

General		
Core Power	MWt	4451 x 1.02
Coolant Pressure	psia	2250 + 30
Nominal Inlet Temperature	deg F	551 + 4
Nominal Outlet Temperature	deg F	617 + 4
Core		
Fuel Rod Lattice	-	17 x 17
Number of Fuel Assembly	-	257
Active Fuel Length	ft	14
Advanced Accumulator		
Number of Accumulator Operating	-	4/4
Accumulator Liquid Volume	ft^3/unit	〔 〕
Accumulator Temperature	deg F	120
Assumed Condition		
Maintenance Outage	-	1 Emergency Power Source
Single Failure	-	1 Emergency Power Source
Containment Spray System		
Number of Spray Pump Operating	-	2/4
Spray Flowrate	GPM/unit	2645
Spray Initiation Time	sec	246
Containment System		
Containment Design Pressure	psig	68
Net Free Volume	ft^3	2.74×10^6
Initial Pressure	psig	2.0
Initial Temperature	deg F	120
Initial Humidity	%	0

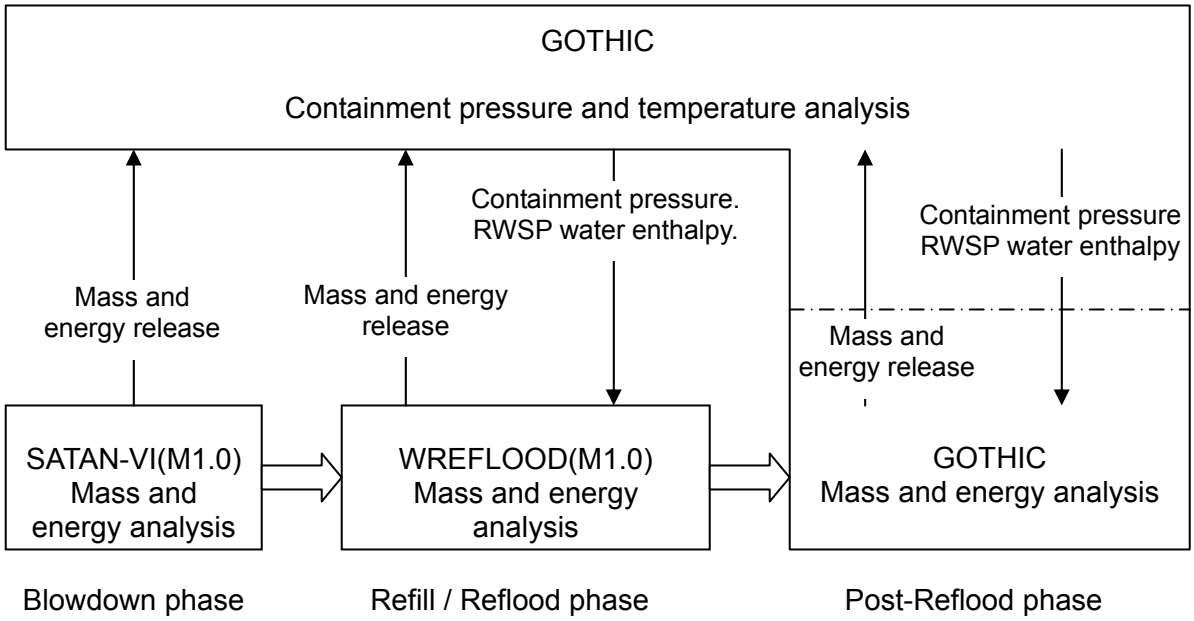

Figure 3-1 The Calculation Code System for Mass and Energy Release and Containment Response Analyses

Figure 3-2 Noding Diagram of SATAN-VI
(Blowdown Phase Mass and Energy Release Analysis)
(Reference 2)

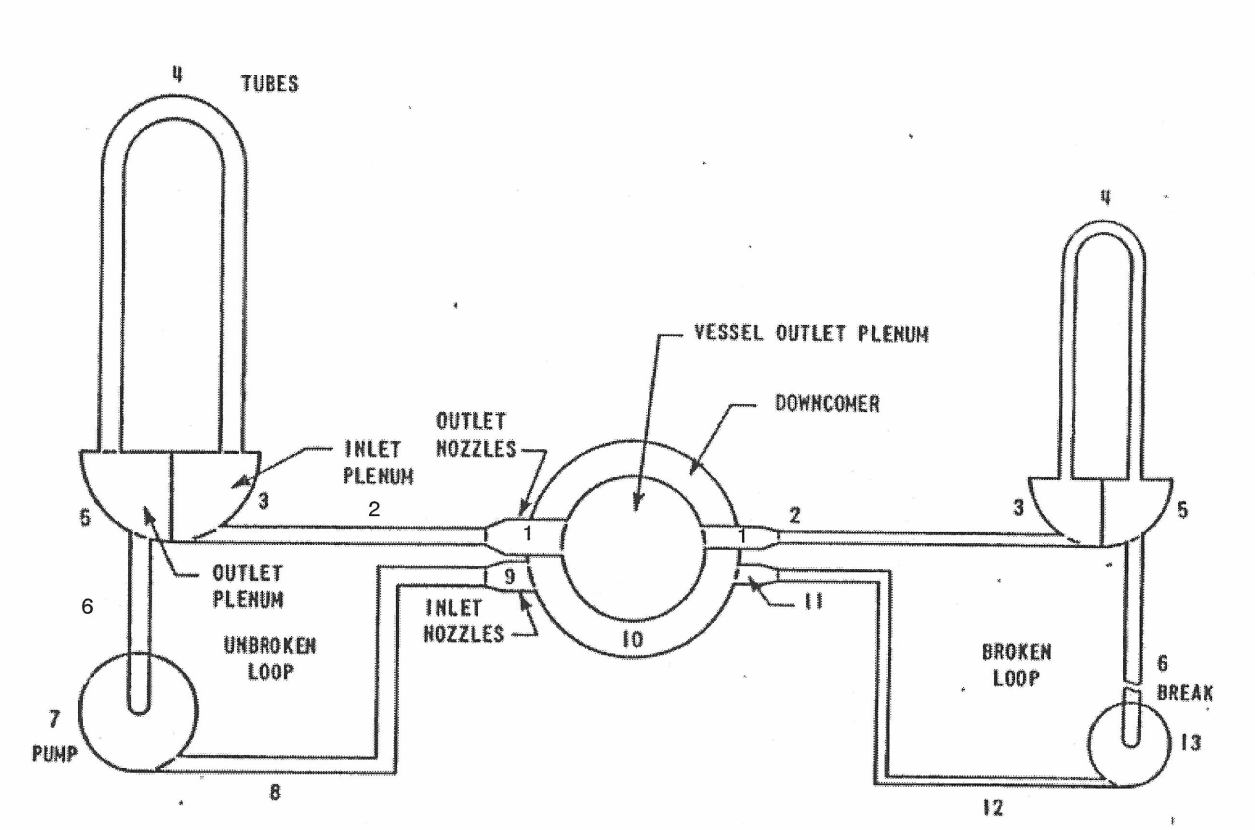

Figure 3-3 Noding Diagram of WREFLOOD
(Reflood Phase Mass and Energy Release Analysis)
(Reference 2)

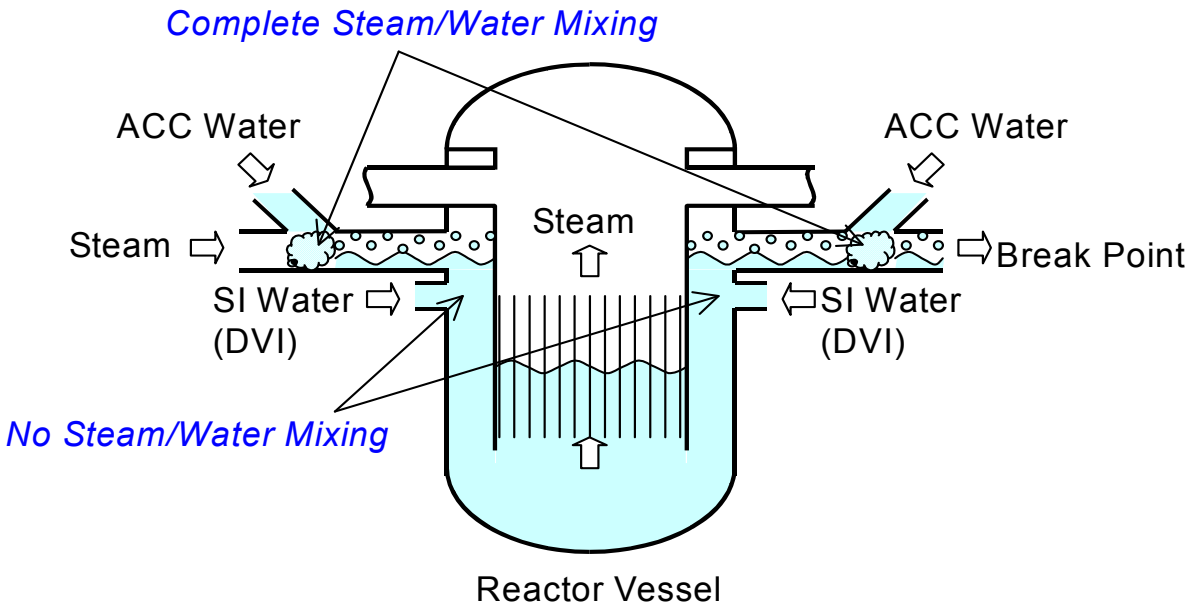

Figure 3-4 Steam/Water Mixing Model for Direct Vessel Injection (DVI)

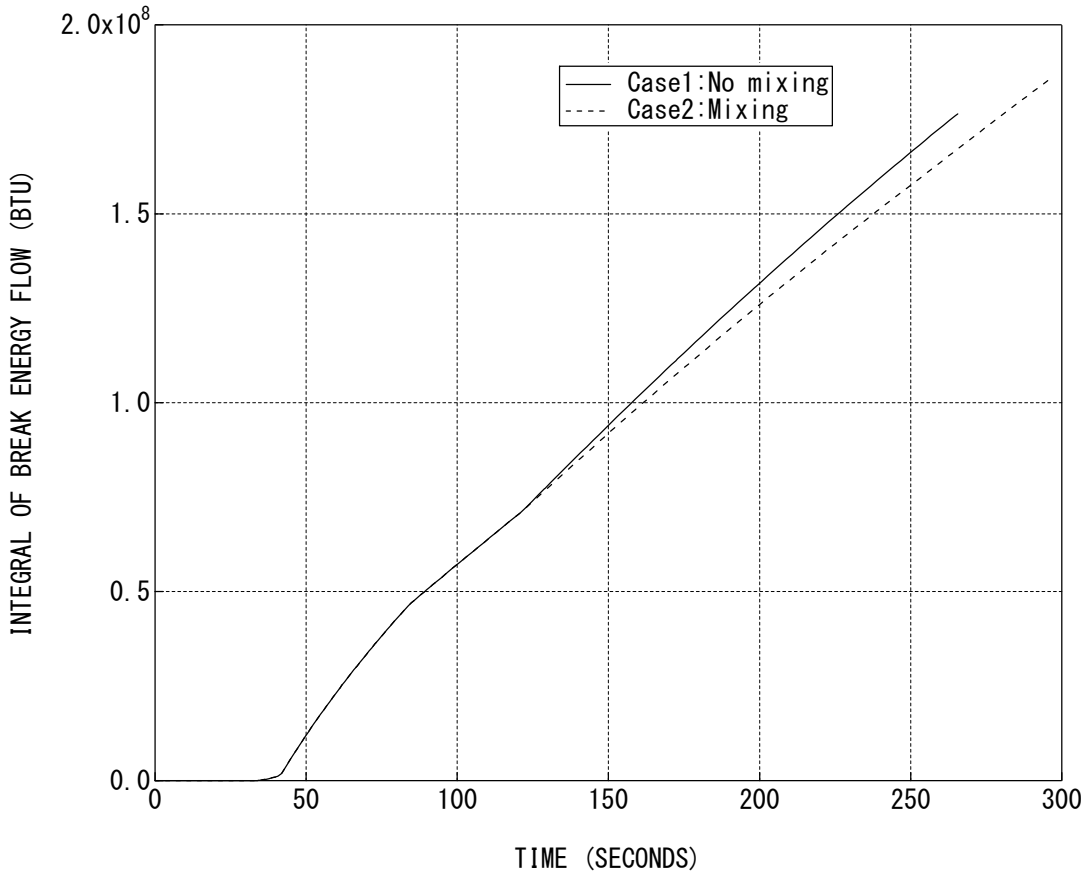

Figure 3-5 Sensitivity Analysis Result about Steam/Water Mixing Model at DVI (Calculated by the WREFLOOD(M1.0) code)

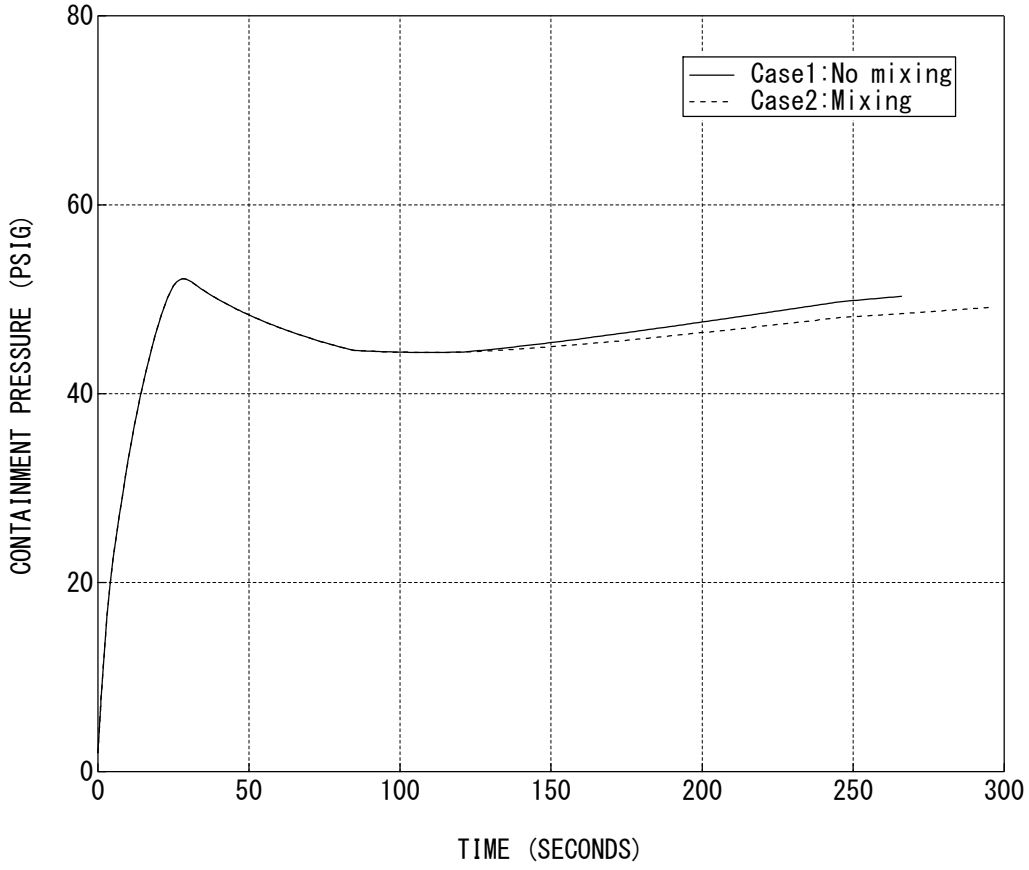

Figure 3-6 Sensitivity Analysis Result about Steam/Water Mixing Model at DVI (Calculated by the GOTHIC code)

Reflood phenomena related to Neutron Reflector

・Metal heat release from thick metal structure

・Affects on Vin (core flooding rate) and Fout (core carry-over fraction)

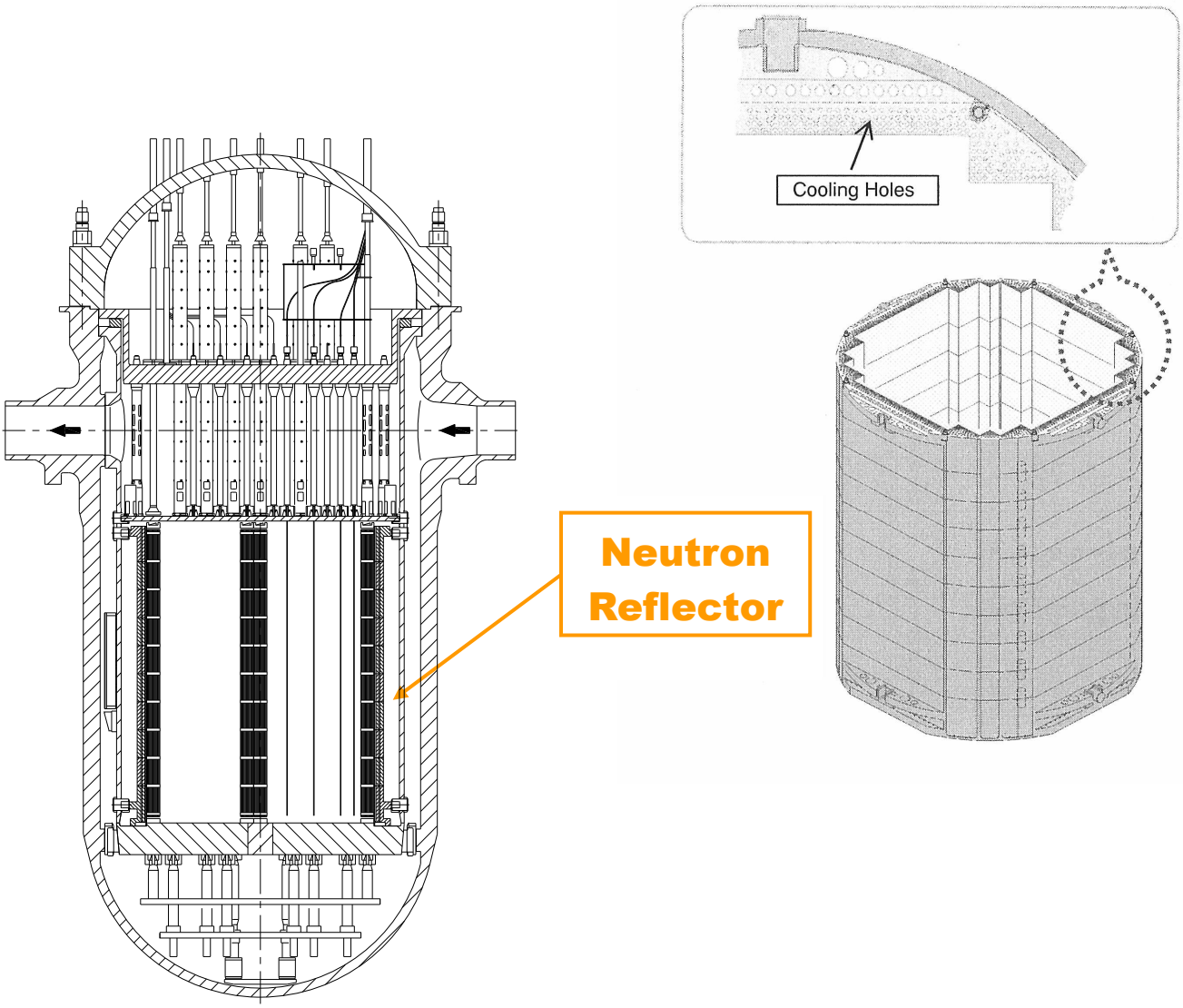

Figure 3-7 Reflood Phenomena Related to Neutron Reflector

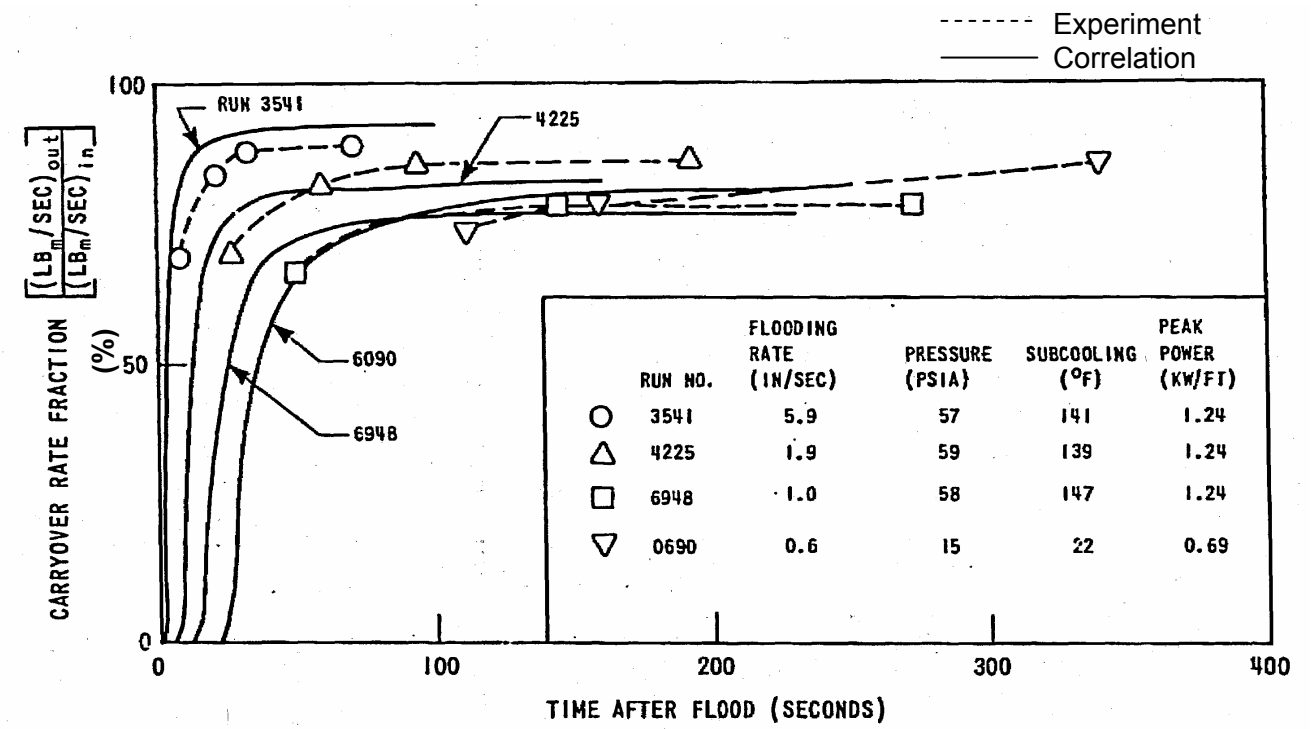

Figure 3-8 Comparison of Carryover Rate Fraction between Correlation and PWR-FLECHT Data

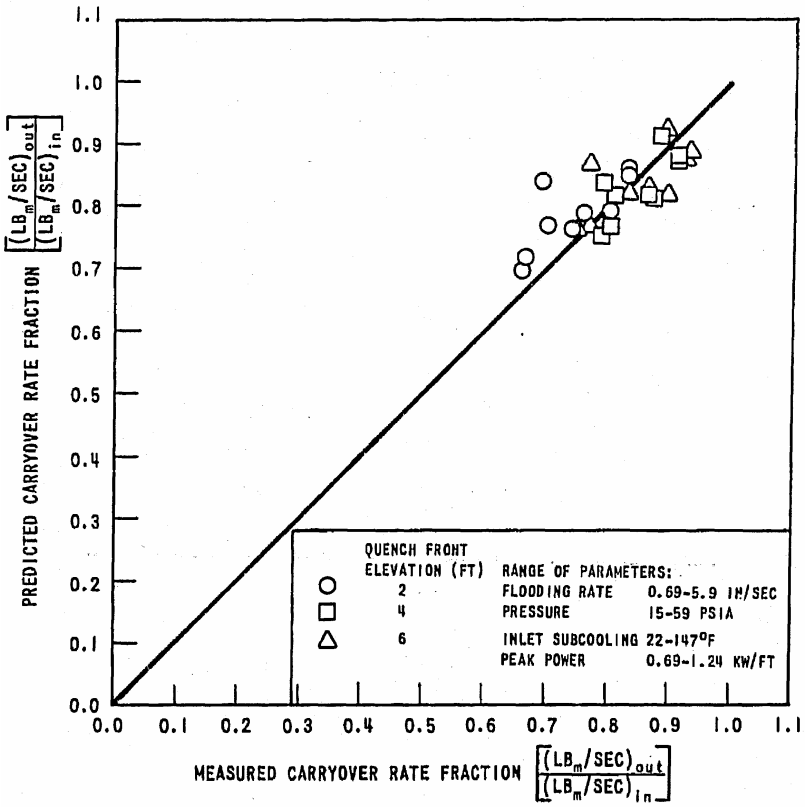

Figure 3-9 Comparison of Measured and Predicted Carryover Rate Fraction

(Both figures are From Reference 4.)

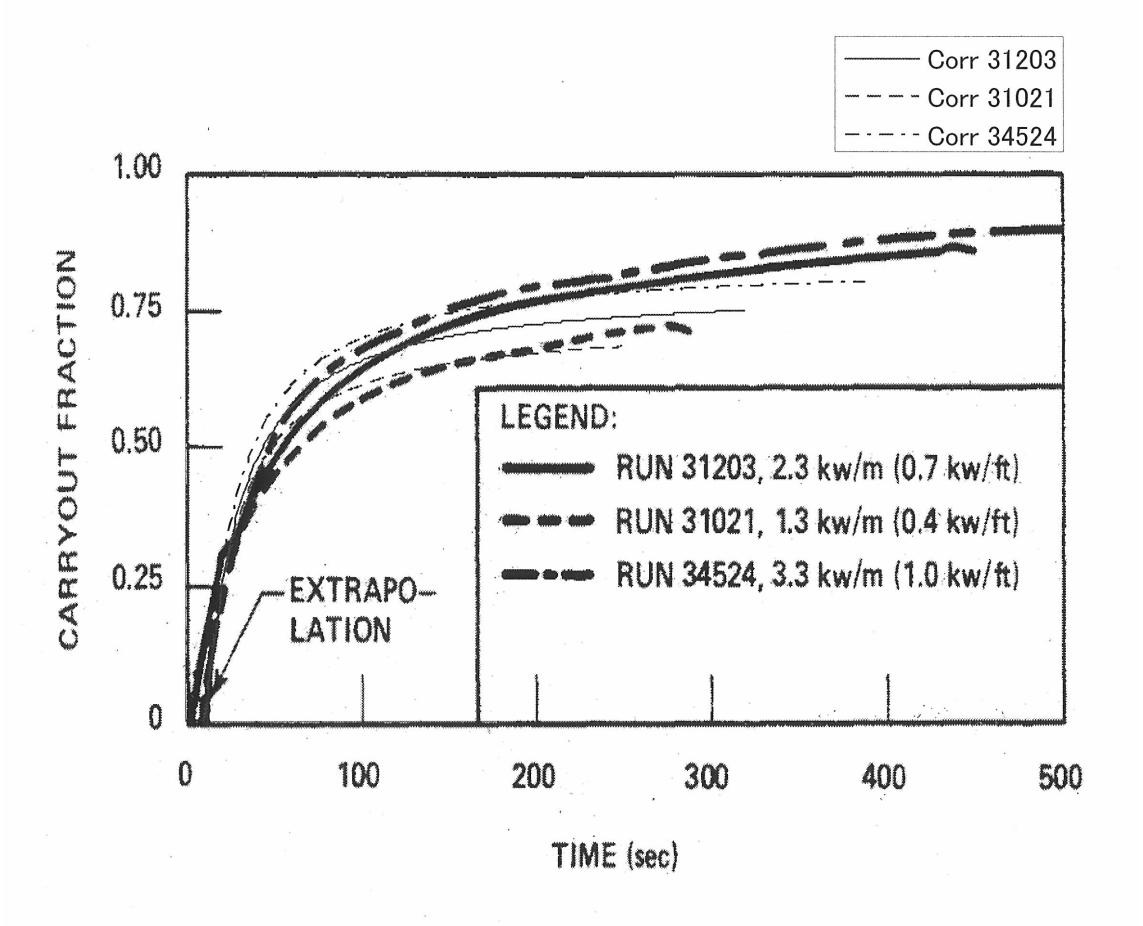

Figure 3-10 Peak Power Effects on Carryout Fraction Comparison of Correlation with FLECHT SEASET Data
(Reference 17)

**Figure 3-11 Noding Diagram of GOTHIC
(Post-reflood Phase Mass and Energy Release Analysis)**

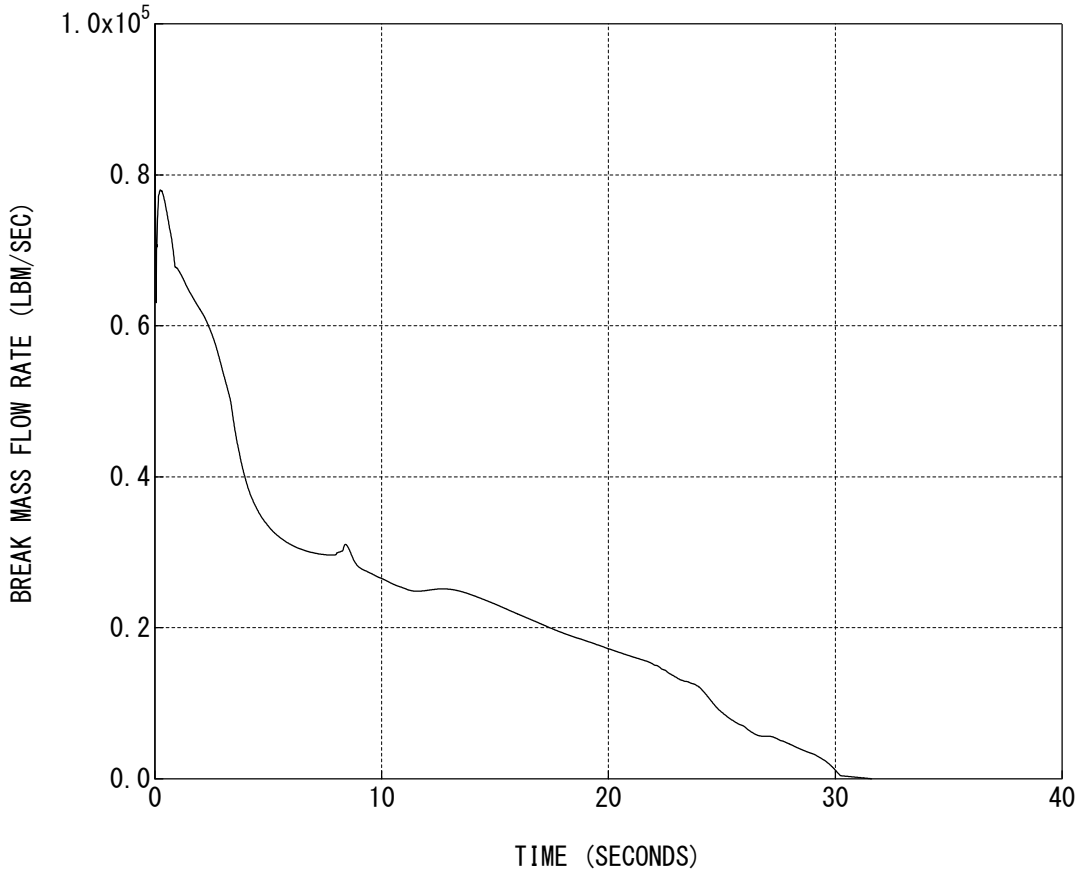

**Figure 3-12 Break Mass Flow Rate (Blowdown Phase)
(Calculated by the SATAN-VI(M1.0) code)**

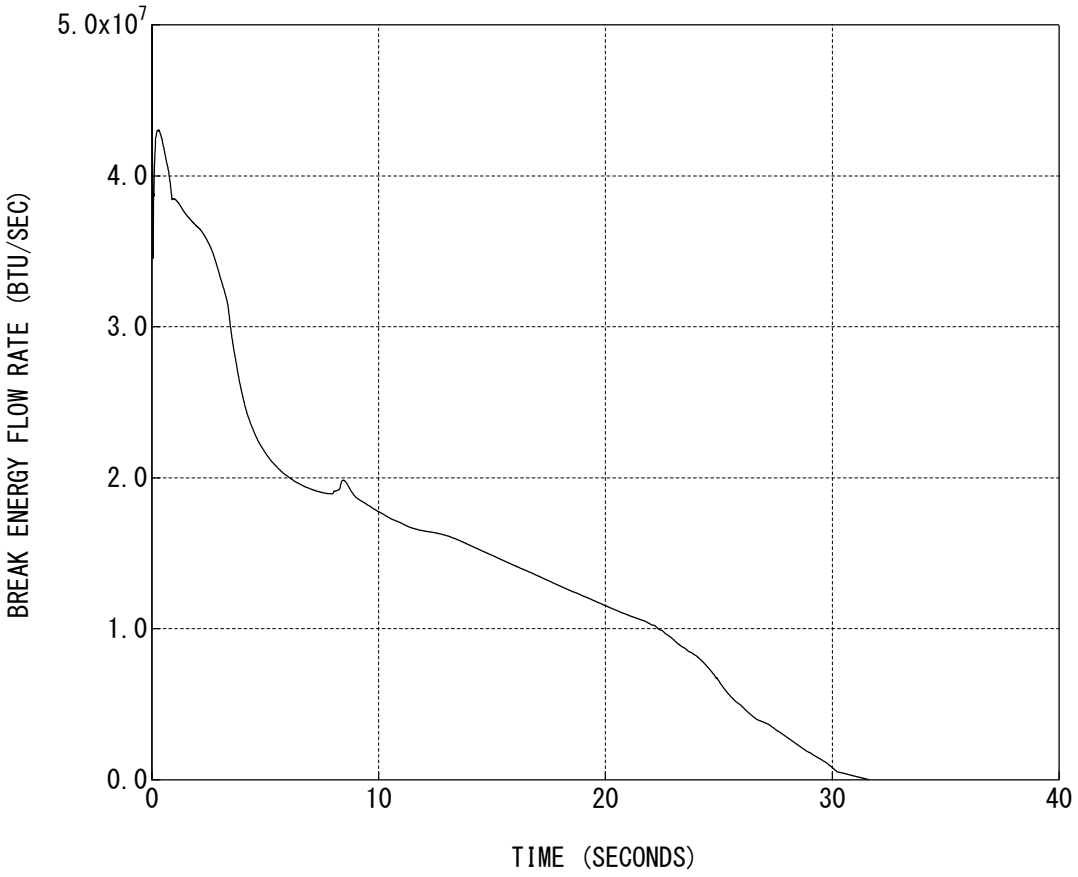

**Figure 3-13 Break Energy Flow Rate (Blowdown Phase)
(Calculated by the SATAN-VI(M1.0) code)**

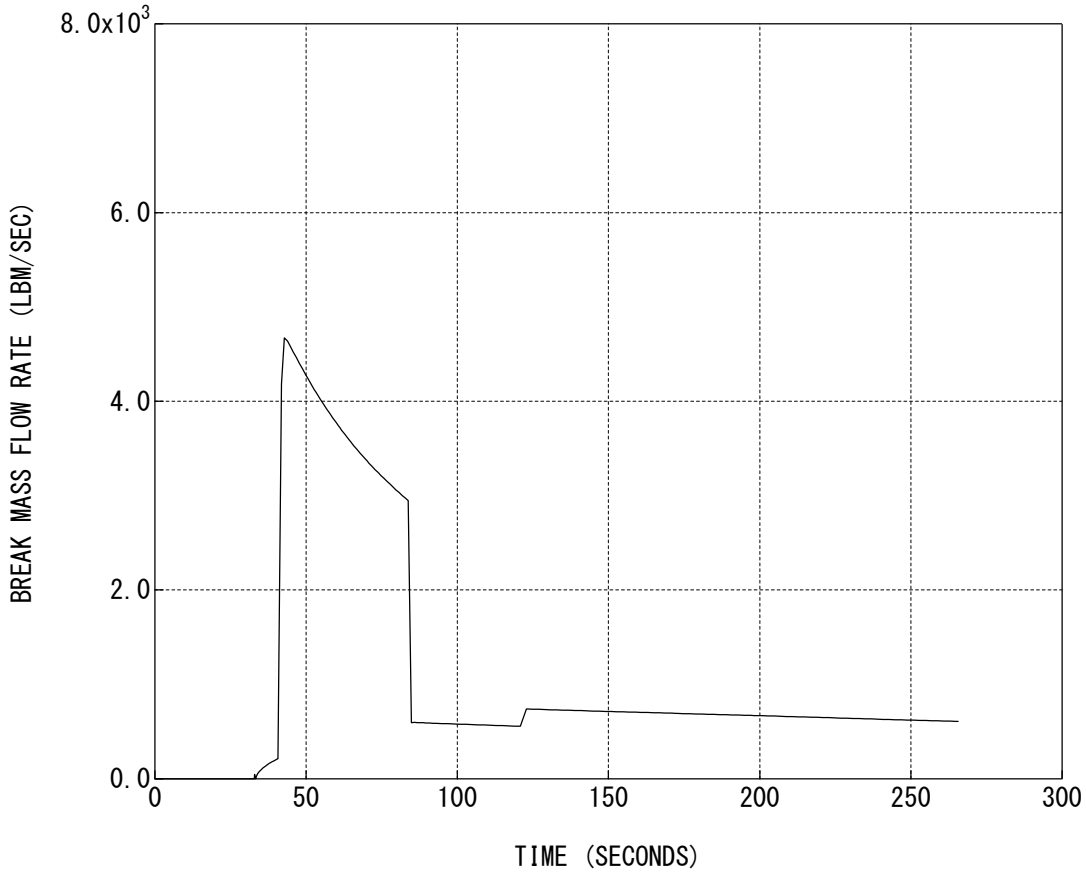

Figure 3-14 Break Mass Flow Rate (Reflood Phase)
(Calculated by the WREFLOOD(M1.0) code)

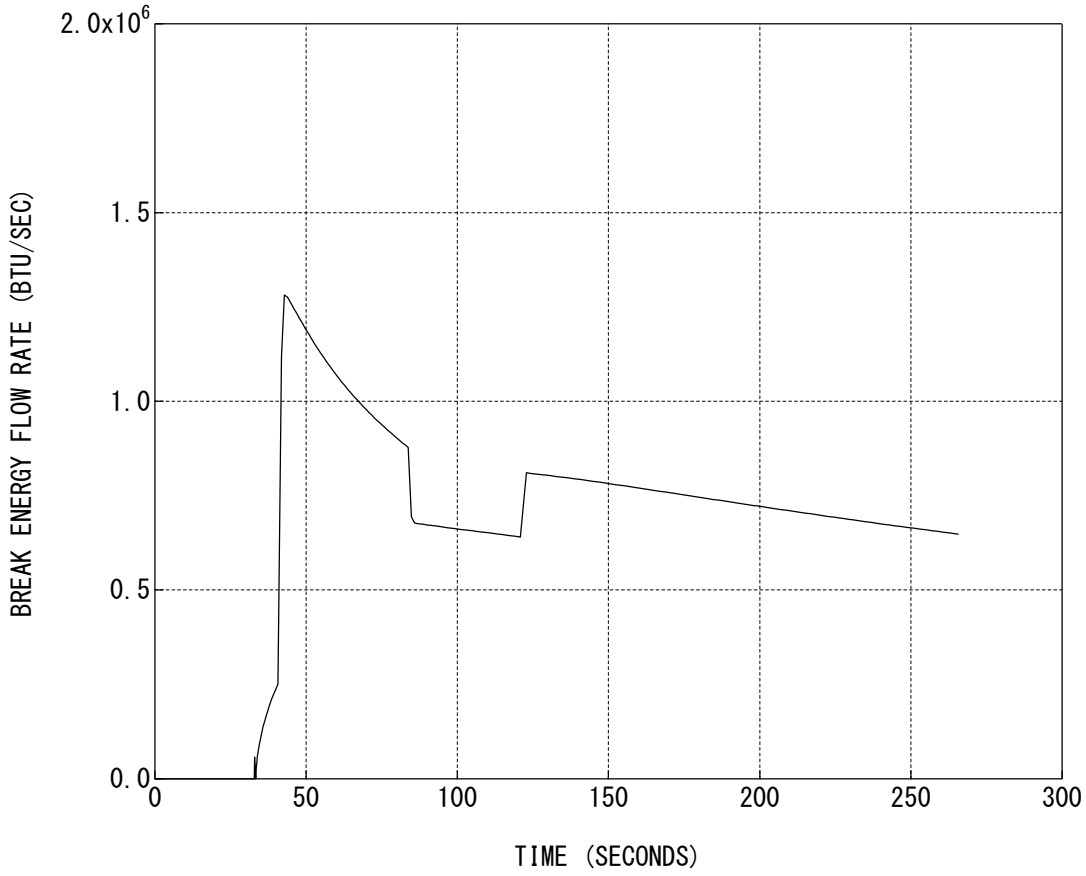

Figure 3-15 Break Energy Flow Rate (Reflood Phase)
(Calculated by the WREFLOOD(M1.0) code)

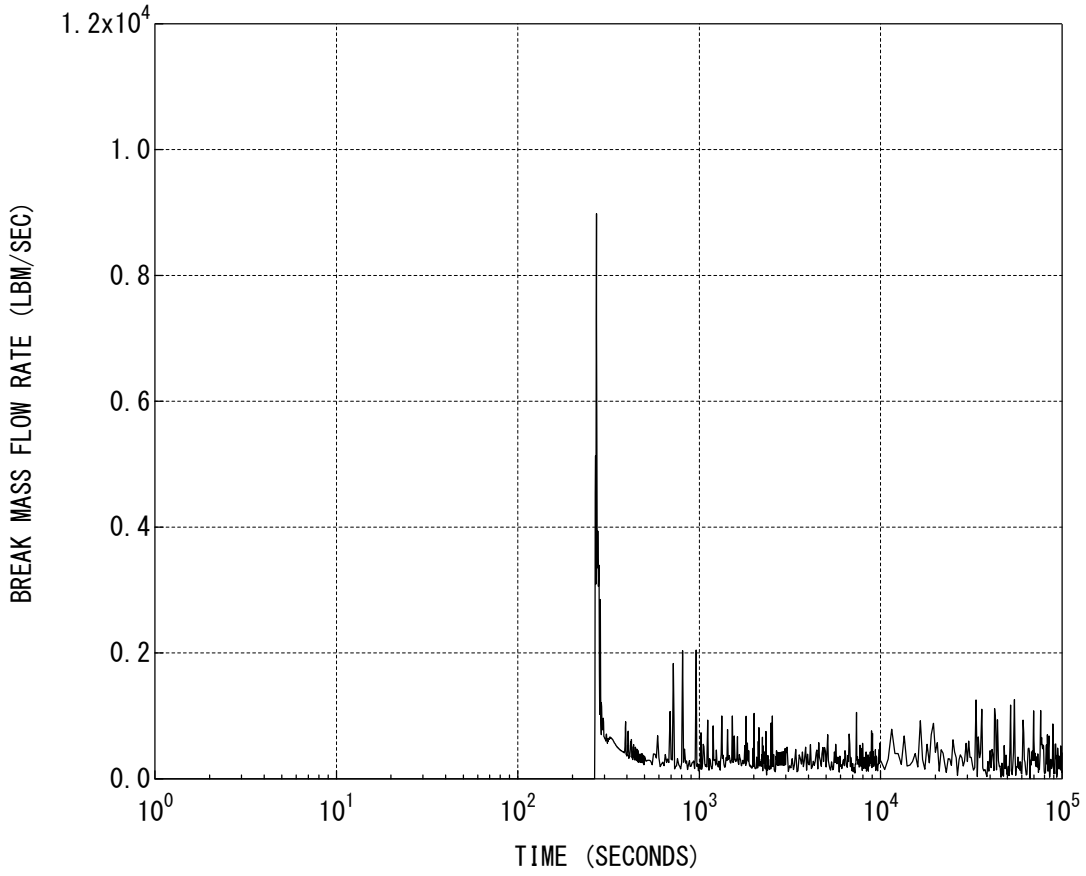

Figure 3-16 Break Mass Flow Rate (Post-reflood Phase)
(Calculated by the GOTHIC code)

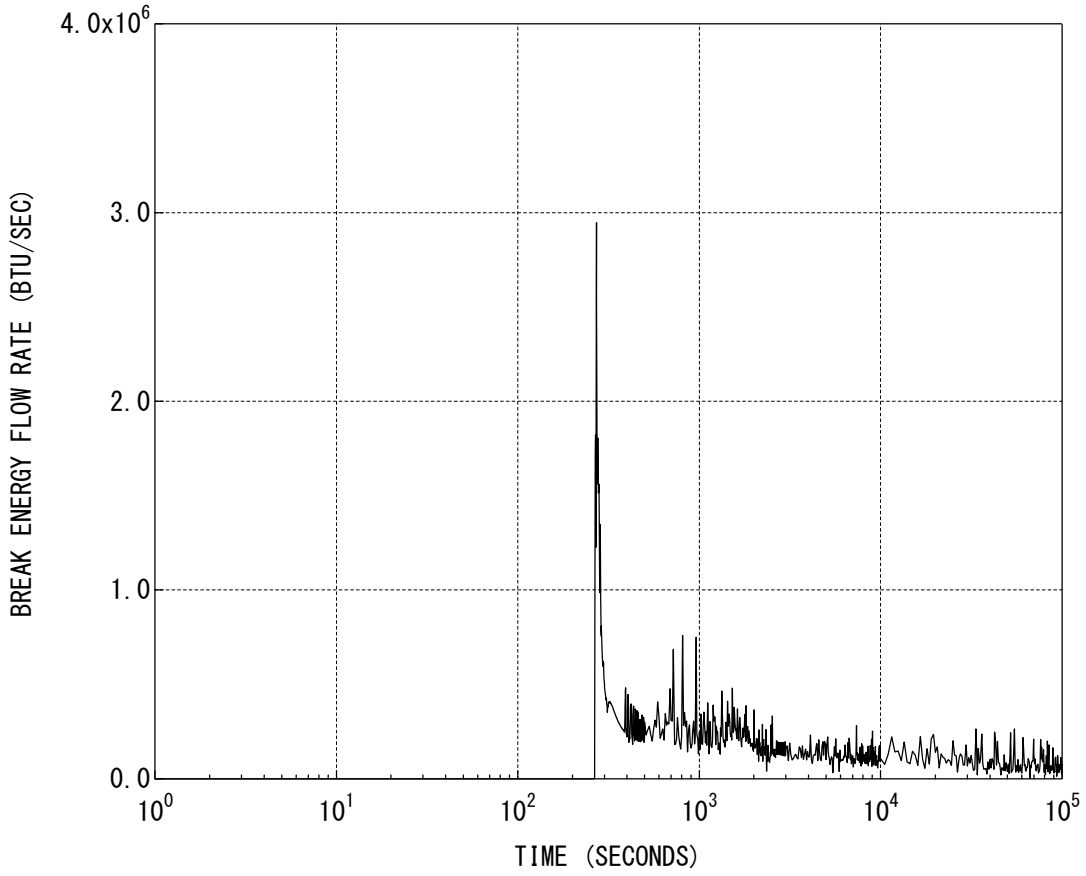

**Figure 3-17 Break Energy Flow Rate (Post-reflood Phase)
(Calculated by the GOTHIC code)**

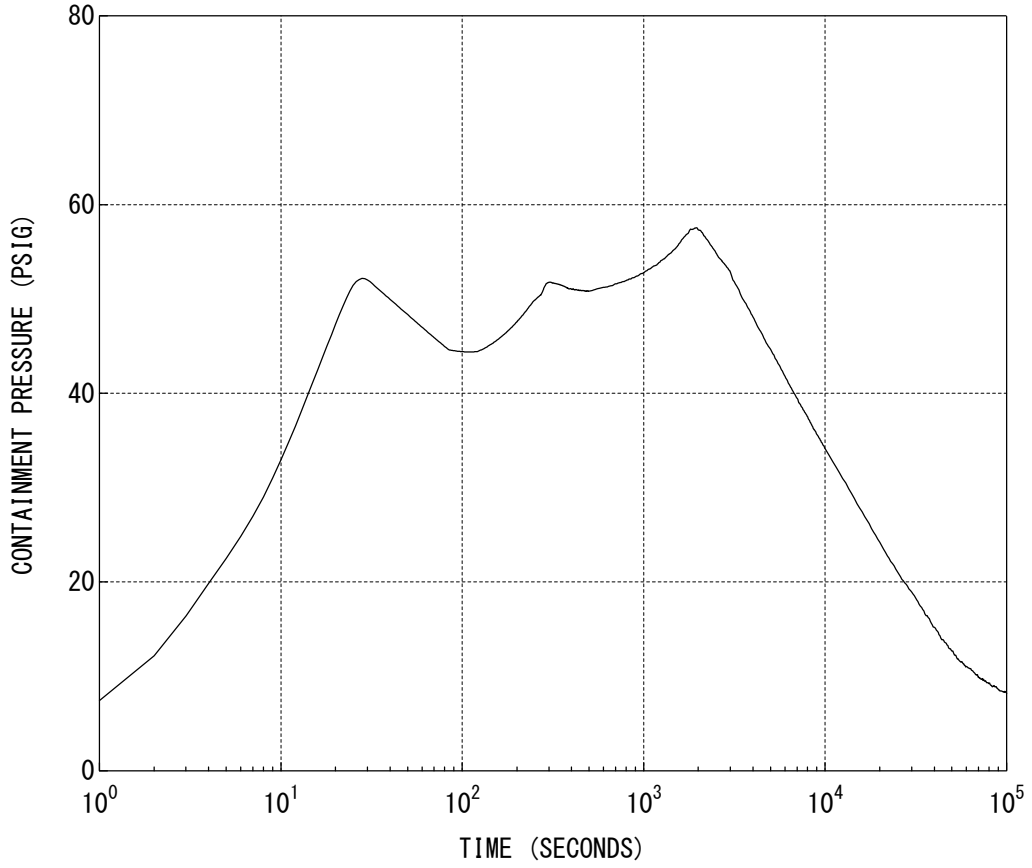

Figure 3-18 Containment Pressure (Calculated by the GOTHIC code)

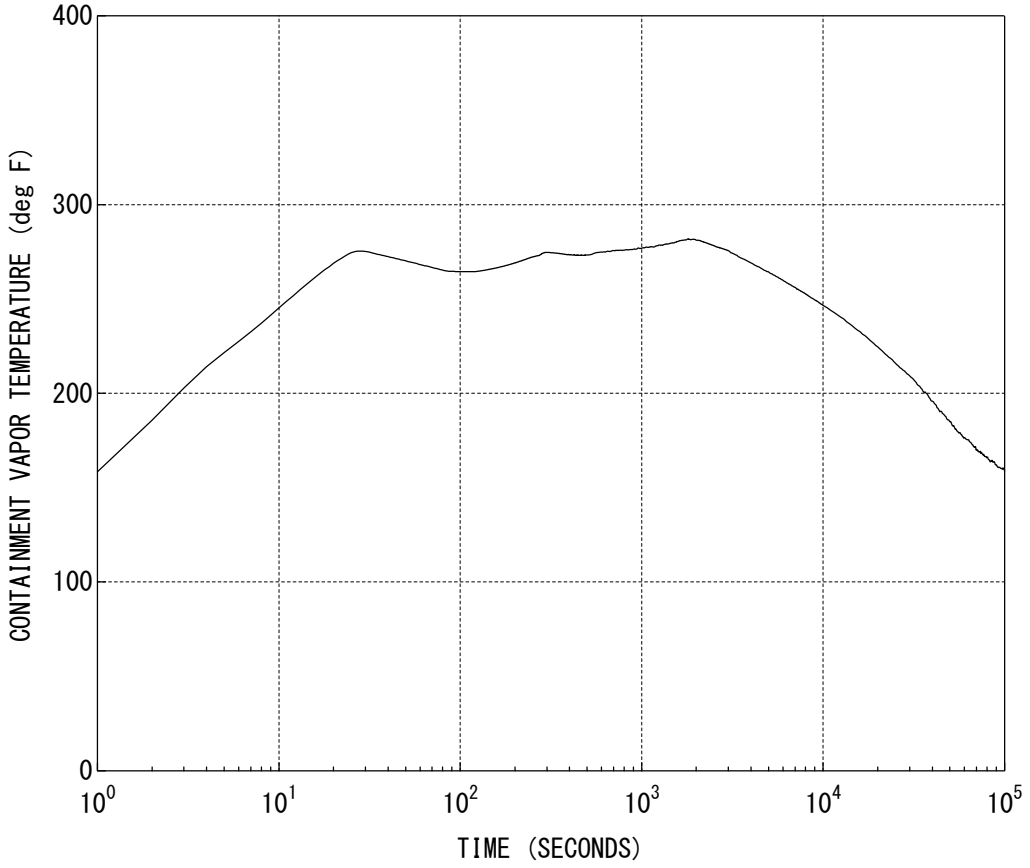

**Figure 3-19 Containment Temperature (Vapor Phase)
(Calculated by the GOTHIC code)**

4.0 CONCLUSIONS

The US-APWR, an advanced PWR with improved design, is retaining many basic features of the existing 4-loop PWR. Therefore the methodology for calculation of mass and energy release to the containment following a design basis loss-of-coolant accident has been developed based on the approved one for the existing PWR with minor modifications to address specific features of the US-APWR.

For Blowdown and Reflood phases, SATAN-VI and WREFLOOD (Reference 2) is utilized with minor modifications for the US-APWR design features, respectively. SATAN-VI was modified for the advanced accumulator and so was WREFLOOD for the advanced accumulator, no steam water mixing of direct vessel injection, the refueling water storage pit and the neutron reflector. All the modifications were confirmed to be appropriate by either test calculations or sensitivity studies.

For post-reflood phase, the GOTHIC code (Reference 8), which has also been already approved by the NRC, is utilized with no modification.

A sample analysis of the US-APWR with the methodology was performed for the large break LOCA, and a reasonable transient behavior was obtained.

The US-APWR mass and energy release analysis methodology is thus established and will be used when determining maximum containment pressure and temperature following a loss-of-coolant accident.

5.0 REFERENCES

1. NUREG-0800 : STANDARD REVIEW PLAN "6.2.1.3 MASS AND ENERGY RELEASE ANALYSIS FOR POSTULATED LOSS-OF-COOLANT ACCIDENTS (LOCAs)"

2. "Westinghouse LOCA Mass and Energy Release Model for Containment Design March 1979 Version," WCAP-10325-P-A, May, 1983.

3. Bordelon, F. M., et. al., "SATAN-VI Program: Comprehensive Space-Time Dependent Analysis of Loss-of-Coolant," WCAP-8302 (Proprietary Version), WCAP-8306 (Non-Proprietary Version), June 1974.

4. Kelly, R.D., et. al, "Calculational Model for Core Reflooding after a Loss-of-Coolant Accident (WREFLOOD Code)," WCAP-8170 (Proprietary Version), WCAP-8171 (Non-Proprietary Version), June 1974.

5. "GOTHIC Containment Analysis Package User Manual, Version 7.2a(QA)," NAI 8907-02 Rev 17, January 2006.

6. "GOTHIC Containment Analysis Package Technical Manual, Version 7.2a(QA)," NAI 8907-06 Rev 16, January 2006.

7. "GOTHIC Containment Analysis Package Qualification Report, Version 7.2a(QA)," NAI 8907-09 Rev 9, January 2006.

8. Letter from Gerald T. Bischof (Virginia Electric and Power Company) to United States Nuclear Regulatory Commission dated November 6, 2006, Transmittal of Approved Topical Report DOM-NAF-3 NP-A, "GOTHIC Methodology for Analyzing the Response to Postulated Pipe Ruptures inside Containment." ADAMS Accession No. ML063190467.

9. Cunningham, J.P. and H.C. Yeh, "Experiments and Correlation for PWR Small Break LOCA Conditions," ANS Transactions, Vol. 17, 1973, p369-370.

10. Lilly, G.P. and L.E. Hochreiter, "Mixing of Emergency Core Cooling Water with Steam: 1/3 Scale Test and Summary," EPRI 294-2, Electric Power Research Institute, June 1975.

11. ANS-5.1-1979, "American National Standard for Decay Heat Power in Light-Water Reactors," August 1979.

12. Letter from N Kalyanam (NRR) to James Scarola (Progress Energy) dated October 12, 2001, "Shearon Harris Nuclear Power Plant Unit 1 – Issuance of Amendment Re: Steam Generator Replacement and Power Uprate (TAC NOS. MB0199 AND MB0782)." ADAMS Accession No. ML012830516.

13. Letter from N. Kalyanam (NRR) to Charles M. Dugger (Entergy Operations) dated July 6, 2000, "Waterford Steam Electric Station, Unit 3 – Issuance of Amendment Re: Reduction in Operable Containment Fan Coolers in the Containment Cooling System (TAC NO. MA6997)." ADAMS Accession No. ML003731172

14. "The Advanced Accumulator," MUAP-07001-R1, January 2007

15. Bajorek, S. M., et al., 1998, “Code Qualification Document for Best Estimate LOCA Analysis,” WCAP-12945-P-A, Volume 1, Revision 2, and Volumes 2 through 5, Revision 1, and WCAP-14747 (Non-Proprietary).
16. F.F. Cadek, D.P. Dominicis, R.H. Leyse, “PWR FLECHT (Full Length Emergency Cooling Heat Transfer) Final Report,” WCAP 7665, April 1971.
17. N. Lee, S. Wong, L. E. Hochreiter, “PWR FLECHT SEASET Unblocked Bundle, Forced and Gravity Reflood Task Data Evaluation and Analysis Report,” NUREG/CR-2256, EPRI NP-2013, WCAP-9891, November 1981.

Appendix A The Advanced Accumulator Model Built into the SATAN-VI Code

The accumulator flow is calculated in subroutine [ ] of SATAN-VI. The advanced accumulator model for US-APWR was built into this subroutine. The configuration of the advanced accumulator model for SATAN-VI(M1.0) is shown in Figure A-1.

It is necessary to estimate the pressure at the flow damper outlet P_o to calculate the resistance coefficient of flow damper K_D.[ ] Therefore it is necessary to define the pressure at the flow damper outlet P_o, that is defined as follows,

[ ] **(A-1)**

The momentum equation in the SATAN-VI code is considered the inertia force (Reference 3).

[ ]

The cavitation factor σ_v is calculated from the flow condition at ACC tank and flow damper outlet as follows,

[ ] **(A-2)**

The flow rate coefficient C_v is calculated using the following correlations obtained from test data which cover the range of applicability for the US-APWR design.

$$\begin{cases} C_v^i = 0.7787 - 0.6889\exp\left(-0.5238\sigma_v^i\right) & \text{(For large flow rate)} \\ C_v^i = 0.07197 - 0.01904\exp\left(-6.818\sigma_v^i\right) & \text{(For small flow rate)} \end{cases} \quad \textbf{(A-3)}$$

C_v is converted to the resistance coefficient of flow damper K_D.

$$K_D^i = 1 \Big/ \left(C_v^i\right)^2 \quad \textbf{(A-4)}$$

[ ] **(A-5)**

[ ]

Total resistance coefficient for ACC system is calculated from K_D and following equation.

$$K_{ACC}=K_D+K_p \quad \textbf{(A-6)}$$

K_{ACC} : Total resistance coefficient of the flow damper and injection piping

The calculation flowchart of advanced accumulator model in SATAN-VI(M1.0) is shown in Figure A-2.

Figure A-1 The Configuration of Advanced ACC Model

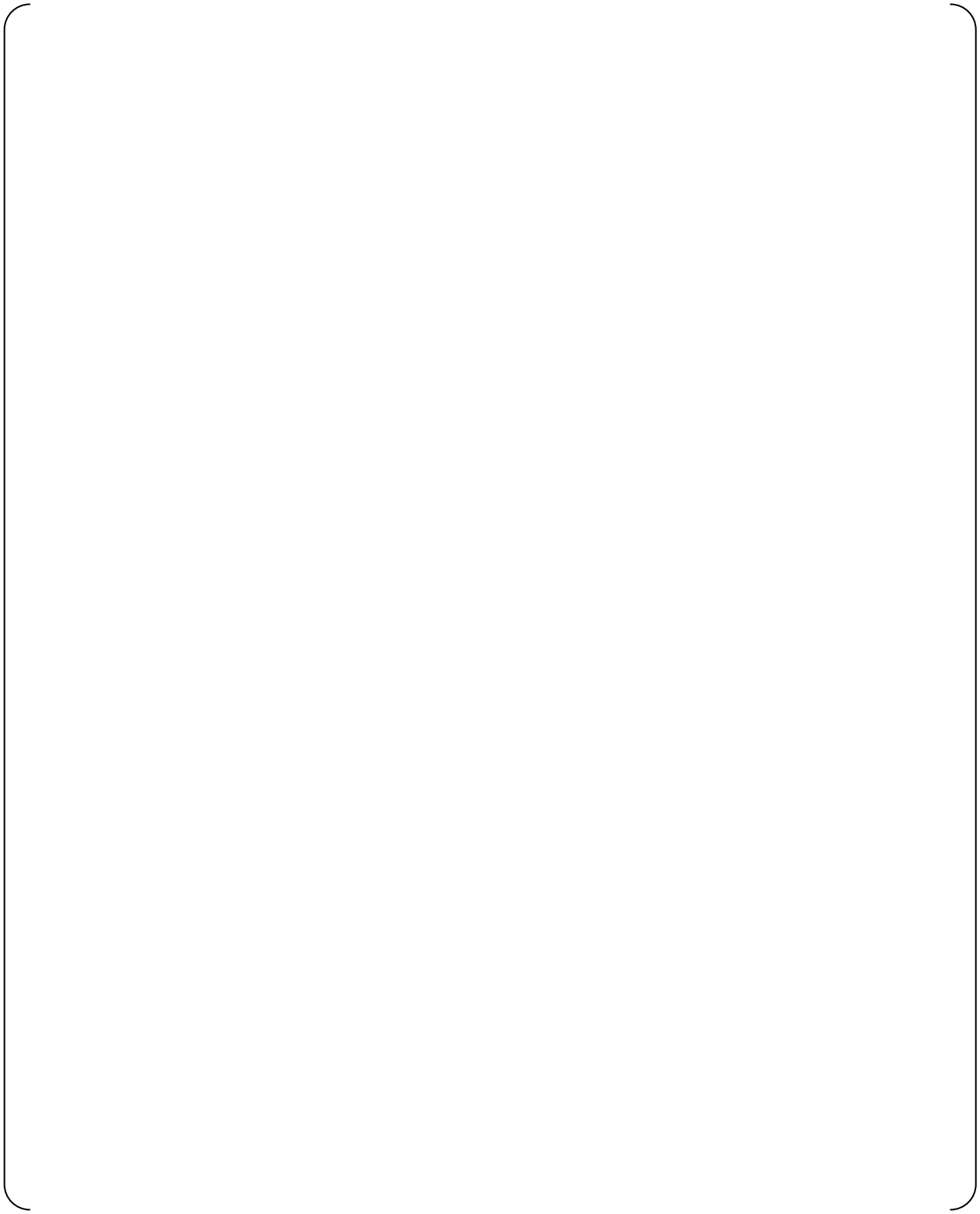

Figure A-2 Calculation Flowchart of Advanced ACC Model in SATAN-VI(M1.0)

Appendix B The Advanced Accumulator Model Built into the WREFLOOD Code

The accumulator flow is calculated in subroutine[ ]of WREFLOOD. The advanced accumulator model for US-APWR was built into this subroutine. The configuration of the advanced accumulator model for WREFLOOD(M1.0) is shown in Figure B-1.

The velocity of the injection piping V_p is calculated as follows,

[ ] **(B-1)**

[ ]Therefore the equation for calculation of V_p is shown in equation B-1.

It is necessary to estimate the pressure at the flow damper outlet P_o to calculate the resistance coefficient of flow damper K_D.[ ]Therefore it is necessary to define the pressure at the flow damper outlet P_o, that is defined as follows,

[ ] **(B-2)**

The cavitation factor σ_v is calculated from the flow condition at ACC tank and flow damper outlet as follows,

[ ] **(B-3)**

The flow rate coefficient C_v is calculated using the following correlations obtained from test data which cover the range of applicability for US-APWR design.

$$\begin{cases} C_v^i = 0.7787 - 0.6889\exp\left(-0.5238\sigma_v^i\right) & \text{(For large flow rate)} \\ C_v^i = 0.07197 - 0.01904\exp\left(-6.818\sigma_v^i\right) & \text{(For small flow rate)} \end{cases} \quad \textbf{(B-4)}$$

C_v is converted to the resistance coefficient of flow damper K_D.

$$K_D^i = 1 \Big/ \left(C_v^i\right)^2 \quad \textbf{(B-5)}$$

[ ]

Total resistance coefficient for ACC system is calculated from K_D and following equation.

$$K_{ACC}=K_D+K_p \quad \textbf{(B-6)}$$

K_{ACC} : Total resistance coefficient of the flow damper and injection piping

The calculation flowchart of advanced accumulator model in WREFLOOD(M1.0) is shown in Figure B-2.

Figure B-1 The Configuration of Advanced ACC Model

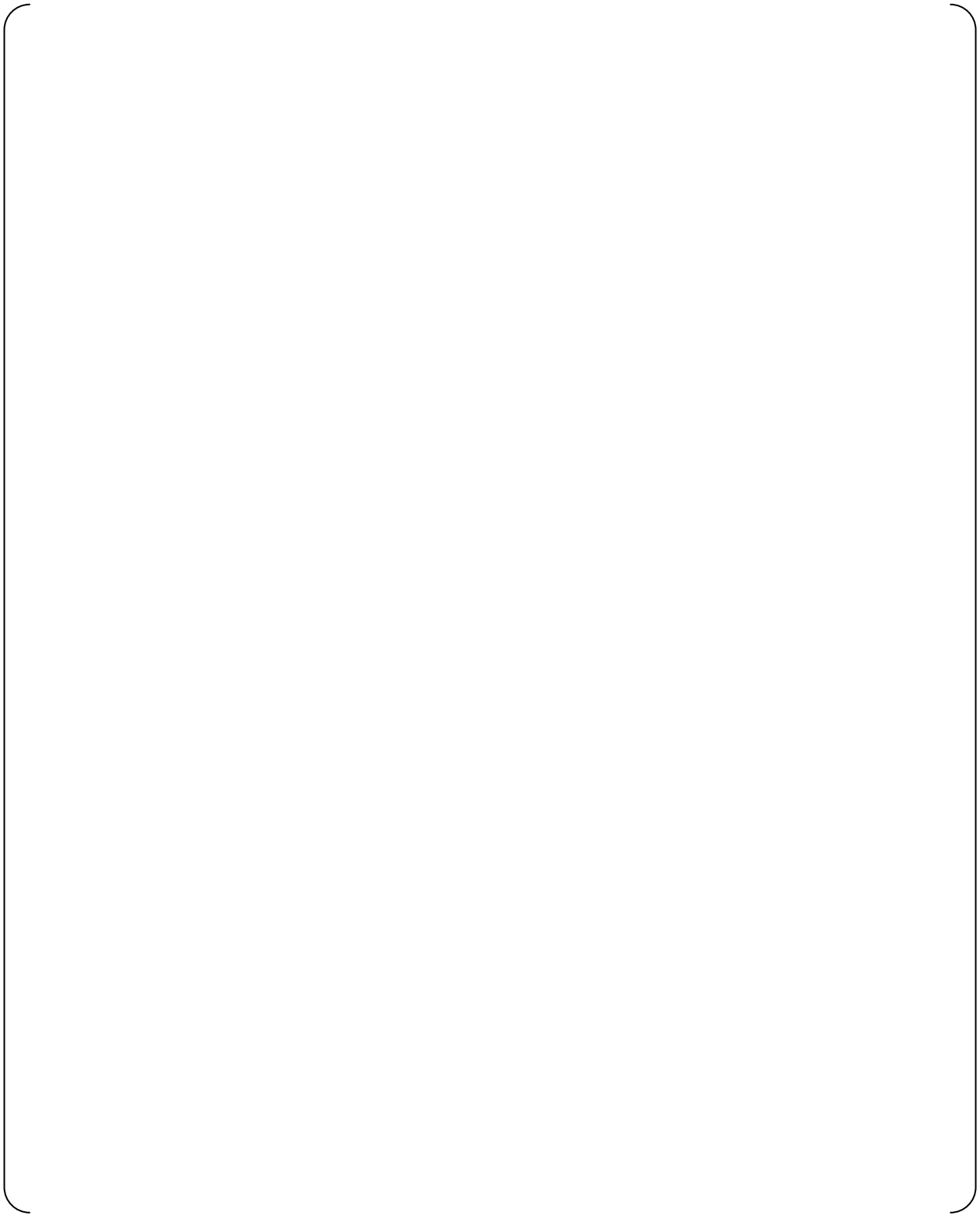

Figure B-2 Calculation Flowchart of Advanced ACC Model in WREFLOOD(M1.0)

Appendix C Validation of the NR Model for the Mass and Energy Evaluation

C.1 Introduction

C.2 Process for the Evaluation

C.3 Results of the Evaluation

C.4 Conclusions

Figure C-1 WCOBRA/TRAC Noding Diagram for the NR

Figure C-2 Inlet and Outlet Pressure of the NR

Figure C-3 Inlet Enthalpy of the NR

Figure C-4 Temperature Distribution of the NR at the End of Reflood

Figure C-5 Integral of Reflooding Rate

Figure C-6 Integral of Reflooding Rate Times Mass Effluence Fraction

Figure C-7 NR Outlet Mass Flow Rate with WCOBRA/TRAC

Figure C-8 Collapsed Liquid Level